NASA TECHNICAL MEMORANDUM

NASA TM X-2935

NASA TM X-2935

AN ANALYTICAL ANALYSIS OF THE DISPERSION PREDICTIONS FOR EFFLUENTS FROM THE SATURN V AND SCOUT-ALGOL III ROCKET EXHAUSTS

by J. Briscoe Stephens, Michael Susko, John W. Kaufman, and C. Kelly Hill

George C. Marshall Space Flight Center
Marshall Space Flight Center, Ala. 35812

NATIONAL AERONAUTICS AND SPACE ADMINISTRATION • WASHINGTON, D. C. • OCTOBER 1973

1. REPORT NO.	2. GOVERNMENT ACCESSION NO.	3. RECIPIENT'S CATALOG NO.
NASA TM X-2935(U)		

4. TITLE AND SUBTITLE	5. REPORT DATE
An Analytical Analysis of the Dispersion Predictions for Effluents from the Saturn V and Scout-Algol III Rocket Exhausts	October 1973
	6. PERFORMING ORGANIZATION CODE M115
7. AUTHOR(S) J. Briscoe Stephens, Michael Susko, John W. Kaufman, C. Kelly Hill	8. PERFORMING ORGANIZATION REPORT #
9. PERFORMING ORGANIZATION NAME AND ADDRESS George C. Marshall Space Flight Center Marshall Space Flight Center, Alabama 35812	10. WORK UNIT NO.
	11. CONTRACT OR GRANT NO.
	13. TYPE OF REPORT & PERIOD COVERED Technical Memorandum
12. SPONSORING AGENCY NAME AND ADDRESS National Aeronautics and Space Administration Washington, D. C. 20546	14. SPONSORING AGENCY CODE

15. SUPPLEMENTARY NOTES

16. ABSTRACT

Predictions of the spatial concentration mapping of the potentially toxic constituents of the exhaust effluents from a launch of a Saturn V and of a Scout-Algol III vehicle utilizing the NASA/MSFC Multilayer Diffusion Program are provided. In the case of the Saturn V, special attention was given to the concentration fields of carbon monoxide with a correlation of carbon dioxide concentrations. The Scout-Algol III provided an example of the centerline concentrations of hydrogen chloride, carbon monoxide, and alumina under typical meteorological conditions. While these results define the specific environmental impact of these two launches under the meteorological conditions existing during launches, they also provide a basis for the empirical monitoring of the constituents of the exhaust effluents of these vehicles.

17. KEY WORDS	18. DISTRIBUTION STATEMENT
Fluid mechanics, Aerospace Effluents Dispersion Modeling, Atmospheric	12

19. SECURITY CLASSIF. (of this report)	20. SECURITY CLASSIF. (of this page)	21. NO. OF PAGES	22. PRICE
Unclassified	Unclassified	85	Domestic, $3.75 Foreign, $6.25

MSFC - Form 3292 (May 1969)

For sale by the National Technical Information Service, Springfield, Virginia 22151

TABLE OF CONTENTS

TABLE OF CONTENTS (Continued)

LIST OF ILLUSTRATIONS

LIST OF ILLUSTRATIONS (Continued)

LIST OF TABLES

ACKNOWLEDGEMENT

This document presents work done by personnel of the Atmospheric Dynamics Branch (S&E-AERO-YA) of the Aerospace Environment Division, Aero-Astrodynamics Laboratory, Marshall Space Flight Center, Alabama. Much credit must be given to Dr. Leonard L. DeVries of the Aerospace Environment Division who contributed greatly to this effort. Messrs. R. K. Dumbauld and Jay R. Bjorklund of the H. E. Cramer Company, Salt Lake City, Utah, made significant contributions to this overall effort.

The review by Langley personnel is appreciated.

AN ANALYTICAL ANALYSIS OF THE DISPERSION PREDICTIONS FOR EFFLUENTS FROM THE SATURN V AND SCOUT-ALGOL III ROCKET EXHAUSTS

J. Briscoe Stephens
Michael Susko
John W. Kaufman
C. Kelly Hill

SUMMARY

The NASA/MSFC Multilayer Diffusion Model is used to predict the dispersion of effluents from the rocket motors during the launch of Apollo 16 on April 16, 1972 at Kennedy Space Center and for a Scout-Algol III vehicle launched on August 13, 1972 at Wallops Island, Virginia. Predictions for two launches were made in real time to gain experience in making such predictions under operational conditions. The analyses of the dispersion of the rocket exhaust effluents from the Saturn V vehicle provide concentration isopleths for large liquid rocket motors. On the other hand, analyses of the effluents resulting from the launch of the Scout-Algol III show ground level concentrations from a small solid rocket motor.

The analyses indicated that ground level concentrations of potential toxic effluents resulting from both launches are well below existing primary and secondary ambient air quality standards.

DEFINITION OF SYMBOLS & TERMS

Symbol		Definition
F_C	=	buoyancy flux
	=	$\dfrac{gQ_F}{\pi\rho c_p T}$
F_I	=	initial buoyancy term
	=	$\dfrac{3gQ_I}{4c_p T\pi\rho}$
FM	=	percentage by weight of pollutant material in the fuel from Table 1
H_L, H_S	=	respective heat contents of liquid and solid fuels
L	=	depth of the surface mixing layer
M	=	molecular weight
P	=	ambient pressure (mb)
$P\{z_{TK}\}$	=	integral of the Gaussian probability function between minus infinity and the top of the K-th layer z_{TK}
	=	$P\left\{\dfrac{z_{TK}-z_{mI}}{\sigma}\right\}$
Q	=	total weight of exhaust products in the stabilized exhaust cloud
	=	$\left(Q_R\right)\left(t_R\left\{z_{mI}\right\}\right)\left(FM\right)$
Q_F	=	rate of heat released by burning fuel
	=	$H_L \circ W_L + H_S \circ W_S$

Symbol		Definition
Q_I	=	effective heat released (cal)
Q_K	=	source strength in units of mass per unit depth of the K-th layer
Q_R	=	fuel expenditure rate from Table 1
T	=	ambient air temperature (^oK)
W_L, W_S	=	respective fuel expenditure rates for liquid and solid fuel
z	=	height above ground of any selected layer
c_p	=	specific heat of air at constant pressure cal/(^oKg)
g	=	gravitational acceleration (9.8 m/sec^2)
r_R	=	initial cloud radius at the surface
$s = \frac{g}{T}\frac{\partial \Phi}{\partial z}$	=	stability parameter
t^*	=	time of layer breakdown
t_H	=	time required for the cloud to reach the stabilization height
t_R	=	time after ignition in seconds
$t_{R_{z_{mI}}}$	=	time in seconds required for the vehicle to reach the height z_{mI} of maximum rise of the ground cloud (obtained from Equation 1)
$\bar{u}$	=	mean wind speed
z	=	height of stabilized cloud
z'	=	midpoint of the K-th layer
	=	$\left(z_{BK} + z_{TK}\right)/2$

Symbol		Definition
z_{BK}	=	height of the base of the K-th layer
z_{BL}	=	height of the base of the L-th layer
z_{L}	=	height in the L-th layer at which the concentration is calculated
z_{mC}	=	maximum height of cloud rise for a continuous source
z_{mI}	=	maximum rise for an instantaneous source
z_{TK}	=	height of the top of the K-th layer
z_{TL}	=	height of the top of the L-th layer
z_{R}	=	altitude above the pad in meters
γ_{C}	=	entrainment constant
γ_{I}	=	entrainment constant
σ	=	standard deviation of the concentration distribution of the stabilized ground cloud
σ_{xK}	=	standard deviation of the alongwind concentration distribution in the K-th layer at distance x
σ_{xLK}	=	standard deviation of the alongwind concentration distribution in the L-th layer for the source originating in the K-th layer
$\sigma_{xo}\{K\}$	=	standard deviation of the alongwind concentration distribution in the K-th layer at cloud stabilization
$\sigma_{yo}\{K\}$	=	standard deviation of the crosswind concentration distribution in the K-th layer at cloud stabilization

Symbol		Definition
$\sigma_{zo}\{K\}$	=	standard deviation of the vertical concentration distribution in the K-th layer at cloud stabilization
σ_{yK}	=	standard deviation of the crosswind concentration distribution in the K-th layer at distance x
σ_{yLK}	=	standard deviation of the crosswind concentration distribution in the L-th layer for the source originating in the K-th layer
σ_{zLK}	=	standard deviation of the vertical concentration distribution in the L-th layer for the source originating in the K-th layer
ρ	=	density of ambient air (g/m^3)
$\frac{\partial\theta}{\partial z}$	=	vertical gradient of ambient potential temperature
χ_p	=	peak or centerline concentration

TERMS

Centerline : The radial vector in the direction of the mean wind direction whose origin is the launch site.

Concentration : is the amount of the effluent present at a specific time. The average concentration is the average amount present during the event.

Dosage : is the measure of the total amount of effluent (time integrated concentration) due to the vehicle launch at a specific location.

Ground Cloud : That cloud of rocket effluents emitted during the initial phase of vehicle launch. This cloud has an ellipsoid shape.

Plume Cloud : The cloud of rocket effluents emitted from th vehicle in flight. This cloud has a cylindrical shape whose height is defined by the vertical thickness of the layer.

TERMS

Potential Temperature (θ)	is the temperature a volume of dry air would have if brought adiabatically from its initial state to the standard pressure of 1000mb.
Quasiadiabatic Layer :	is a layer in which the vertical potential temperature gradient is zero or less.
Stable Layer :	is a layer in which the vertical potential temperature gradient is positive.

SECTION I. INTRODUCTION

The NASA/MSFC Multilayer Diffusion Program has been utilized to predict the dispersion of the effluents from the booster during the launches of the Apollo 16 (Apollo Saturn 511) on April 16, 1972 at Kennedy Space Center and of a Scout vehicle launched on August 13, 1972 at Wallops Island, Virginia.

The National Environmental Policy Act of 1969 and the April 23, 1972, guidelines of the Council on Environmental Quality require statements covering proposed federal actions that might affect the environment. Such statements are required for assessing the environmental impact of the Space Shuttle and other NASA space vehicle rocket motor effluents. Development of quantitative procedures for estimating the space vehicle rocket motor toxic fuel hazard has been underway for over a decade at the NASA Marshall Space Flight Center. Computerized and graphical procedures for estimating toxic fuel hazards have been developed [1] utilizing a Lagrangian model for estimations in the troposphere. In addition to estimates of atmospheric transport, dispersal and decay of all airborne toxic material released as a result of normal launch operations, estimates must also be provided for cases involving fuel spillage, vehicle abort, or vehicle destruct situations.

Universally accepted and adequately validated prediction techniques for the rocket motor effluent problem are not available, and much uncertainty exists concerning very important aspects of the problem, such as the amount and composition of the rocket engine effluents, and their dispersal and transport in the atmosphere. The available atmospheric measurements to ascertain the reliability of the description of rocket effluent dispersion models in the atmosphere are sparse and of questionable accuracy. On the other hand, the requirements for estimating toxic fuel hazards clearly exist in order to establish special constraints on operations, test, and launch activities to assure allowable concentrations of these effluents will not be exceeded. The need for implementing a program for monitoring rocket engine exhaust effluents has been recognized for many years. As a result of informal discussions between representatives of NASA Headquarters, Marshall Space Flight Center, Langley Research Center, and Kennedy Space Center, it became apparent that a NASA inhouse rocket engine effluent prediction and measurement program was desirable, possible, and feasible.

The announcement by the President on January 5, 1972, that the United States should proceed at once with the development of the Space Shuttle Program resulted in renewed interest in the dispersion of potentially toxic engine effluents. The subsequent decision by NASA

to power the first stage of the Shuttle by Solid Rocket Motors added significant importance to the problem, since their major exhaust constituents contain large amounts of carbon monoxide (CO), hydrogen chloride (HCl), and aluminum oxide (Al_2O_3), all of which may be classified as air pollutants and toxic.

To initiate the program of predicting and measuring downwind concentrations of exhaust effluents, such predictions and measurements of the ground cloud and upper altitude plume generated by the Saturn V vehicle and, subsequently, a Scout vehicle were made. Our objective is to provide lead information for Solid Rocket Motors Programs whereby the various investigators may gain an insight into the behavior of the transport of the toxic exhaust effluents, and to improve the accuracy of various empirical parameters utilized in our dispersion calculations. To this end, we have selected two different actual examples -- a large liquid rocket engine, the Saturn V, and a small solid rocket motor, the Scout -- to provide an initial baseline for the investigations of the dispersive effluent transport.

The various descriptions for the models of dispersive transport of the rocket exhaust available with the NASA/MSFC Multilayer Diffusion Program required, because of the various phases of plume development and changing environment conditions, are summarized in the next section. The detailed formulations for the algorithms employed in the models along with a toxicity criteria are afforded in the appendix. Section III and IV give a detailed summary of the effluent transport predictions for the launch of Apollo 16 and for the launch of a Scout vehicle, respectively.

SECTION II. NASA/MSFC MULTILAYER DIFFUSION MODEL

The spatial description, in terms of concentration and dosage, of the dispersive transport of effluents from a discrete source is afforded by the NASA/MSFC Multilayer Diffusion Model. Specifically, this application of the model is for the prediction of toxicity distribution associated with the rocket exhaust effluents emitted during the launch of a space vehicle in order to assess the resulting environmental impact. The dispersive description accorded by the Multilayer Diffusion Model is initiated at the point where the cloud of effluents reaches thermodynamic equilibrium with the environment and therefore depends strongly on the kinematic and thermodynamic profiles of the atmospheric conditions along with a knowledge of the exhaust effluents present in the cloud.

The initial considerations in this section are given to the techniques of establishing the spatial location of the ground cloud equilibrium (see definitions). Secondly, a general discussion of the Lagrangian dispersion of a point source is given. The final discussion in this section explains how the Multilayer Diffusion Model incorporates the general diffusion description to account for the two stages of exhaust emission and accounts for the environmental effects. The significant mathematical expressions supporting these discussions have been included in Appendix I, II, and III.

a. Altitude of Cloud Equilibrium

The effluent cloud rise relations are employed to determine at what altitude the ground cloud reaches equilibrium with the environment. The importance of this location is that it serves as the origin of the dispersive description. This equilibrium point is chosen as the origin in order to eliminate complex thermodynamic considerations and to limit the problem to solely kinematics.

The burning of rocket engines results in the formation of a cloud of hot exhaust products which subsequently rises and entrains ambient air until an equilibrium with ambient conditions is reached. For normal launches, this cloud is formed principally by the forced ascent of hot turbulent exhaust products that have been deflected laterally and vertically by the launch pad hardware and the ground surface. The height at which this ground cloud stabilizes is determined by the vehicle type and atmospheric stability. The vehicle type determines whether a continuous or instantaneous source model is required. In the instantaneous source model, spherical entrainment is assumed; that is, the entrained ambient air enters the exhaust cloud uniformly from all directions. In the continuous source model, cylindrical entrainment

is assumed; that is, the entrained ambient air enters the cloud uniformly only on the sides of the cylinder and not the ends. Thus, this terminology -- continuous or instantaneous source -- in reference to the cloud rise model does not imply the duration of the exhaust cloud, as it does in the diffusion model, but only implies the form of the entrainment process. The entrainment process is a function of the residence time of the vehicle on the pad. Experience to date indicates that the buoyant rise of exhaust clouds from normal launches of solid-fueled and small liquid-fueled vehicles is best predicted by using a cloud rise model for instantaneous sources; the cloud rise for large liquid-fueled vehicles is best predicted by the use of a cloud rise model for continuous sources. While no cloud rise data are available for on-pad aborts, cloud rise data from static tests of liquid-fueled rockets indicates that the use of a cloud rise model for continuous sources is appropriate.

Each of the models for cloud height is subdivided into two categories to account for the atmospheric temperature lapse rate. The model assumes that the atmosphere is either quasi-adiabatic or stable. Here the quasi-adiabatic is where the adiabatic atmosphere is the limit, which means that the potential temperature difference ($\Delta\theta$) is zero or less, where the potential temperature difference is given by $\Delta\theta = \theta_{\text{max cloud height}} - \theta_{\text{surface}}$. If this potential temperature difference is positive, then the atmosphere is treated as stable. Since in most cases of interest there will be an inversion layer present, the stable cloud rise formula is the normally utilized relation.

b. Generalized Diffusion Model

The generalized diffusion model describes the kinematic transport -- in terms of the temporal and spatial levels of concentration and dosage -- of the exhaust effluent constituents assuming the effluent cloud is in equilibrium with the environment. A Lagrangian model is assumed, where volumetric cloud expansion is about a reference point in a homogeneous fluid. For diagnostic and interpretation flexibility, this model is formated in a modular form for both concentration and dosage.

The generalized concentration model for a nearly instantaneous source is expressed as the product of five modular terms:

$$\text{Concentration} = \{\text{Peak Concentration Term}\} \times \{\text{Alongwind Term}\} \times \{\text{Lateral Term}\} \times \{\text{Vertical Term}\} \times \{\text{Depletion Term}\} ;$$

whereas, the generalized dosage model for a nearly instantaneous source is defined by the product of four modular terms:

$$\text{Dosage} = \{\text{Peak Dosage Terms}\} \times \{\text{Lateral Term}\}$$

$$\times \{\text{Vertical Term}\} \times \{\text{Depletion Term}\}$$

Thus, the mathematical description for the concentration and dosage models permit flexibility in application to various sources and for changing atmospheric parameters while always maintaining a rigorous mass balance.

Two obvious differences exist. First, the peak concentration term refers to the concentration at the point x, y = 0, z = H (where x is the wind direction and H is any height) and is defined by the expression

$$\frac{Q}{(2\pi)^{3/2}\sigma_x\sigma_y\sigma_z}, \qquad (1)$$

where Q is the source strength and σ_i is the standard deviation of the concentration distribution in the i^{th} direction; whereas, the peak dosage term is given by

$$\frac{Q}{2\pi\bar{u}\sigma_y\sigma_z}, \qquad (2)$$

where $\bar{u}$ is the mean wind speed. The second difference between these models is that the concentration contains a modular alongwind term to account for downstream temporal effects not considered in the dosage model. The alongwind term affords an exponential decay in concentration as a function of: cloud transit time, concentration distribution and the mean wind speed.

The lateral term - which is common to both models - is another exponential decay term, and is a function of the Gaussian spreading rate and the distance laterally from the mean wind azimuth. The vertical term - again common to both models - is a rather complex decay function since it contains a multiple reflection term for the point source which stops the vertical cloud development at the top of mixing layer and eventually changes the form of the vertical concentration distribution from Gaussian to rectangular. The last modular in both models is the depletion term. This term accounts for the loss of material by simple decay processes, precipitation scavenging or gravitational settling.

Each of the modular terms in these two relations is heavily dependent upon empirical parameters. For this reason, it is necessary to perform reliable investigations of as many rocket launches as possible and to perform controlled investigations of rocket exhausts experiments to insure the maximum reliability in these empirical parameters. This will in turn afford a more accurate dispersion description from these models.

c. The Description of the Models in the NASA/MSFC Multilayer Diffusion Model

The normal launch environment will usually involve an atmospheric structure comprised of several horizontal meteorological layers with distinctive wind velocity, temperature, and humidity regimes between the surface and a 5 kilometer altitude. Large horizontal spatial variation in these meteorological parameters may also occur in the surface layer as a consequence of changes in terrain or land-water interfaces, which is accounted for by the diffusion model. The general diffusion model for the concentration (Equation 1) and the dosage (Equation 2) assumes an expanding volume about a moving point of reference in a homogeneous environment.

To overcome the obvious shortcomings of the general diffusion model but to stay within the established bounds of classical fluid mechanics [2], a multiple layer concept is introduced to cope with the vertical and horizontal atmospheric gradients. Here, the general diffusion model is applied to individual horizontal layers in which the meteorological structure is reasonably homogenous and independent of the neighboring layers. These layers have boundaries which are placed at points of major discontinuities in the vertical profiles of wind velocity, temperature, and humidity. Since the Multilayer Diffusion Model has imposed the general restriction of layer independence (no flux of particles or gases entering or leaving an individual layer), special provision must be made for spatial changes in the horizontal meteorology and for gravitational settling or precipitation scavenging. In addition, the type of source within a layer must be considered; that is, whether there is a ground cloud source or a plume cloud source (see definitions).

The NASA/MSFC Multilayer Diffusion Model has six models (Figure 1) which account for three categories of dispersive constraints: The source distribution, the environmental effects and the depositional effects. This flexibility is required to deal with the stages of the development of the exhaust cloud and the complex potentially varying meteorological conditions. These models can be used alone to describe all the environmental layers or in superimposed combinations where variations in layer meteorology require different modeling. For

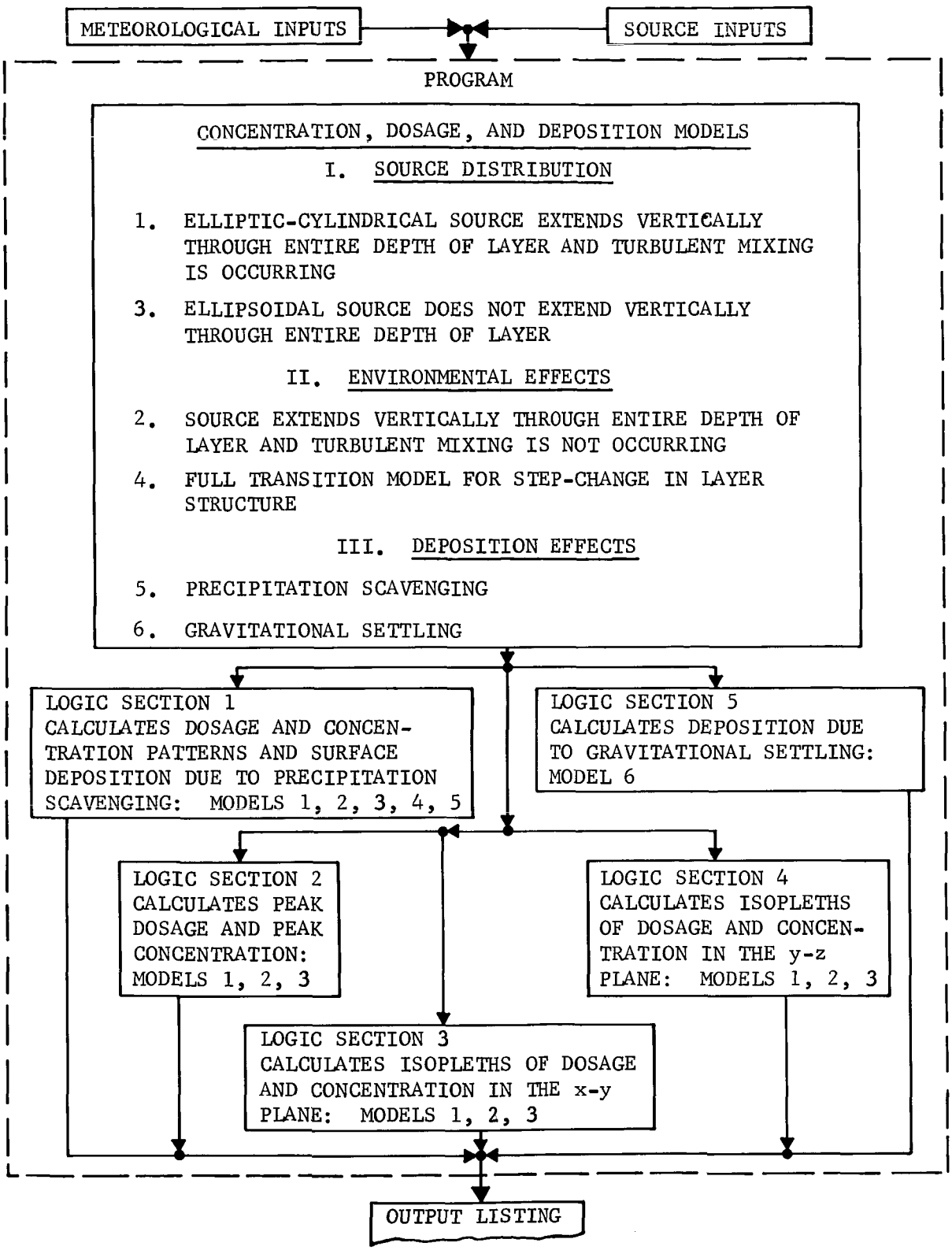

FIGURE 1. BLOCK DIAGRAM OF THE COMPUTER PROGRAM FOR THE NASA/MSFC MULTILAYER DIFFUSION MODEL.

the introductory overview, however, these combinations will not be considered. The primary output of all models is a mapping of the regimes of the concentration and dosage isopleths and centerline profiles for concentration and dosage.

The fundamental category of dispersive constraints is the source distribution. The two distributions are:

1. The elliptic-cyclindrical source which assumes a two dimensional Gaussian distribution in the x-y plane and a uniform distribution in the vertical direction.

2. The ellipsoidal source which assumes a three-dimensional Gaussian distribution.

Model 1 is for the elliptic-cylindrical source whose vertical expansion is constrainted by the layer boundaries -- thus has only a two dimensional expansion in the horizontal plane due to turbulence mixing. This model is normally used to describe the rocket's inflight plume cloud.

Model 3 is for the ellipsoidal source and is assumed to expand in all three dimensions as the effluents are propagated downstream. When the ellipsoidical source reaches the top of the mixing layer, the distribution of the constituents is reflected back into the expanding vertical distribution. On the other hand, that fraction not lost in surface deposition is also reflected back in a similar manner. After sufficient mixing, the ellipsoidal distrituion becomes a elliptic-cylindrical distribution (Model 1). While Model 3 is normally used to describe the dispersion of the rocket's ground cloud, it could be used to model upper air explosions. The formulation for Model 3 has been provided in Appendix II.

The second category is environmental effects. The two effects are:

1. No turbulence mixing in the upper atmosphere.

2. Changes in meteorological conditions as the constituents are transported downstream.

Model 2 is the same as Model 1 except it is assumed that there is no turbulent mixing. This implies that the exhaust material just meanders along the layer without dispersing. While the Model 2 is not generally used, movies of rocket firings clearly show that under some special meteorological conditions this model is required. While the Multilayer Diffusion Model is general in applicability, it is specific in meteorological parameters and launch description.

Model 4 updates the diffusion model with changes in meteorological conditions and structure which can occur as the constituents propagate downstream. This model assumes that the vertical concentration of material has become uniform throughout each layer when a step-change in the meteorological conditions is introduced, resulting in the destruction of the original layer boundaries and the formation of new layer boundaries. The concentration fields which exist at this time are treated as new sources. In those new layers which now comprise more than one old layer, the old concentration is mapped as two independent concentration sources and then superimposed for the resulting concentration and dosage mappings.

The third category of dispersive constraints includes the deposition due to:

1. Precipitation scavenging

2. Gravitational settling

Model 5 accounts for precipitation scavenging. An example of where Model 5 must be used is in solid rocket launches during the occurrence of rain, because the HCl will be scavenged by the rain. Model 6 describes the ground deposition due to gravitational settling of particles or droplets. Wind shears are incorporated in this model to account for the effect of the settling velocity of the particulate matter. There are two forms for the source in this model; namely:

1. The source that extends vertically through the entire layer with a uniform distribution -- this is the same source model as used with Models 1 and 2, and

2. A volume source in the K-th layer -- this is the same source model as used with Model 3.

Model 6 is very important in the analysis of the settling of Al_2O_3 particles released in solid rocket firings.

The treatment of cold spills and fuel leaks that occur near ground level requires a continuous source, but the models that have been considered so far are for discrete sources; therefore, the models must be adapted for the use in predicting concentration-dosage levels downwind from continuous sources.

The layer of the environment influenced by the ground-level spills and leaks can be treated as homogeneous; therefore, the general formula for concentration and dosage (Equations 1 and 2) presented in the initial discussion would be applicable if spills and leaks are treated as continuous sources. To visualize this adaption for these

formulas, assume a source cloud with a concentration distribution that implies a given dosage at a point for this cloud; that is, the dosage per event. If there are a number of similar clouds, discretely spaced, then for each cloud we obtain a dosage for each cloud whose sum corresponds to the total dosage for the entire event.

In the limit as the spacing between clouds approaches zero and the number of clouds becomes large, the discrete source approaches a continuous source whose concentration is the point dosage per unit time. The relation for the continuous concentration, which follows directly from this argument, is

Concentration = (Peak Concentration) x (Lateral Term)

x (Vertical Term x (Depletion Term)

$$\chi_{peak} = \frac{Q}{2\pi\, \bar{u}\, \sigma_y \sigma_z t_R} \quad , \tag{3}$$

where Q is the source strength, $\bar{u}$ is the mean wind speed, σ_i is the concentration distribution in the i-th direction and t_R is the release time.

The Lateral Term, Vertical Term, and the subset of equations defining σ_y and σ_z are the same as for the point source dosage (Equation 2). The continuous dosage is then the continuous concentration times the release time.

In summary, the Multilayer Diffusion Model is composed of six submodels. Models 1 and 3 are designed to distinguish between the two sources of toxic cloud formation -- the ground cloud during the initial launch phase (Model 3) and the plume cloud after the initial launch phase (Model 1). From the stand point of environmental impact, the description of the fields of the ground deposition of materials from the ground cloud is of primary significance -- this description is afforded by Model 3. Generally, this model is employed in the surface layer, but can be employed in any layer where the source does not extend through the entire layer.

Model 2 was designed to account for a lack of turbulent mixing which can occur in the upper atmosphere. Model 4 is employed when a change in meteorological condition occurs during the downstream transport of the cloud. In the event of rain, the precipitation scavenging -- both of gases and particles -- can be accounted for in Model 5. The fallout of particulate matter on the ground is the domain of Model 6. These six submodels form the basic set of equations which are available to treat the diffusion problem. To model a specific

launch of a vehicle, it is necessary to blend these equations together and adjust the model parameters to the specific meteorological conditions of the launch, to the specific terrain around the launch site and to the specific vehicle being launched; thus the degree of complexity in the diffusion model.

SECTION III. PREDICTIONS OF THE DISPERSIVE TRANSPORT OF SATURN V ENGINE EXHAUST EFFLUENTS IN THE TROPOSPHERE (APRIL 16, 1972)

Concentration mappings of the exhaust effluents from the launch of the Apollo 16 mission (Apollo Saturn 511) at 1754 Universal Time (UT) (1254 EST) from Kennedy Space Center obtained from the NASA/MSFC Multilayer Diffusion Model are presented in this section. Since the calculation of the exhaust effluent dispersions presented in this report are limited to altitudes below 18 km, only the exhaust effluents from the first stage (S-1C) of this Saturn V have an effect upon the concentration mapping and the effluents from the remaining stages can be neglected here.

The two important input parameters in the Multilayer Diffusion Model are the vehicle fuel properties and the meteorological conditions; these input parameters will be discussed as an introduction to the actual model parameters employed and the predictions obtained.

a. Saturn V (S-1C) Engine Exhaust Effluents

It has been established theoretically and from observations that low altitude clouds of engine exhaust and entrained gases are formed during the launch of the S-1C booster [3]. In the case of the S-1C vehicle, these clouds regularly rise and stabilize at an altitude of about 2 km, depending upon meteorological conditions. The engine exhaust effluents contained in this cloud are produced during the period from rocket ignition to the time that it ascends to the altitude as which the exhaust ground cloud stabilizes. For a cloud stabilization altitude of two km, the ground cloud contains the exhaust effluents produced during approximately the first 43 seconds of engine ignition, or about 6.524×10^5 kg (Table I). The composition of these liquid engine exhaust effluents at engine exit and after reaction with the atmosphere consists primarily (99.9 percent, see Table II) of water vapor (H_2O), carbon monoxide (CO) and carbon dioxide (CO_2). Of these gases, the only two that are considered toxic are carbon monoxide and carbon dioxide (see Appendix II, Toxicity Criteria). The stabilized ground cloud from Apollo 16 contained about 2.85×10^5 kg of carbon monoxide [4].

The single-start F-1 engine, with a fixed thrust of 6.8×10^6 N, uses liquid oxygen as the oxidizer and RP-1 as the fuel. Water, hydrocarbons, and other carbon compounds make up the major bulk of the engine exhaust. Eight minutes before lift-off, 5.02×10^2 kg/sec (8,000 gallons/minute) of water are sprayed into the trench (Figure 2). At 2 minutes before lift-off, 1.26×10^3 kg/sec (20,000 gallons/minute) of water are sprayed onto the mobile launcher, launch pad, and into the trench for cooling purposes. Six seconds after ignition, the F-1

TABLE I

EXHAUST MATERIALS EMITTED AS A FUNCTION OF ALTITUDE FROM THE S-1C STAGE

Altitude Range (km)	Range Time at Top of Layer (sec)	Exhaust Material Emitted (kilograms)
0-2	36**	5.460×10^5
2-4	49	1.690×10^5
4-6	58	1.170×10^5
6-8	66	1.040×10^5
8-10	72	7.800×10^4
10-12	78	7.800×10^4
12-14	83	6.500×10^4
14-16	88	6.400×10^4
16-18	92	5.200×10^4
18-20	96	5.200×10^4
20-22	100	5.200×10^4
22-24	104	5.200×10^4
24-26	107	3.900×10^4
26-28	110	3.900×10^4
28-30	113	3.900×10^4
30-40	128	1.950×10^5
40-50*	140	1.456×10^5
50-60	151	1.144×10^5
60-70	160	9.360×10^4

*Layer in which IBECO occurs; only four engines burn after T + 135.96 seconds.

**Total effluent calculations based on 43 seconds in that ignition occurs at T - 7 seconds.

TABLE II

F-1 EXHAUST COMPOSITION

Component	Weight Percent at Exit	Estimated Weight Percent After Reaction w/Atmosphere *
H_2	1.13	
OH	.22	
H_2O	26.6	27.5
O	.005	
O_2	.011	
CO	42.2	43.6
CO_2	27.8	28.8
CHO	.002	
H	.022	
HC	1.60	
Particulates	.0575	.0575
NO_x	0	.0005

Hydrocarbons and particulates result primarily from turbine exhaust. Hydrocarbons are expected to burn when mixed with primary flow and atmosphere.

Primary exhaust products are based on theoretical data. Imperfect mixing is the primary mechanism which might cause the measured composition to differ from theoretical.

Measured turbine exhaust composition agrees very well with predicted composition but no data have been located to confirm the expected reaction with primary flow and atmospheric oxygen.

*These estimates were made by S&E-AERO-AT, Marshall Space Flight Center, Alabama, National Aeronautics and Space Administration.

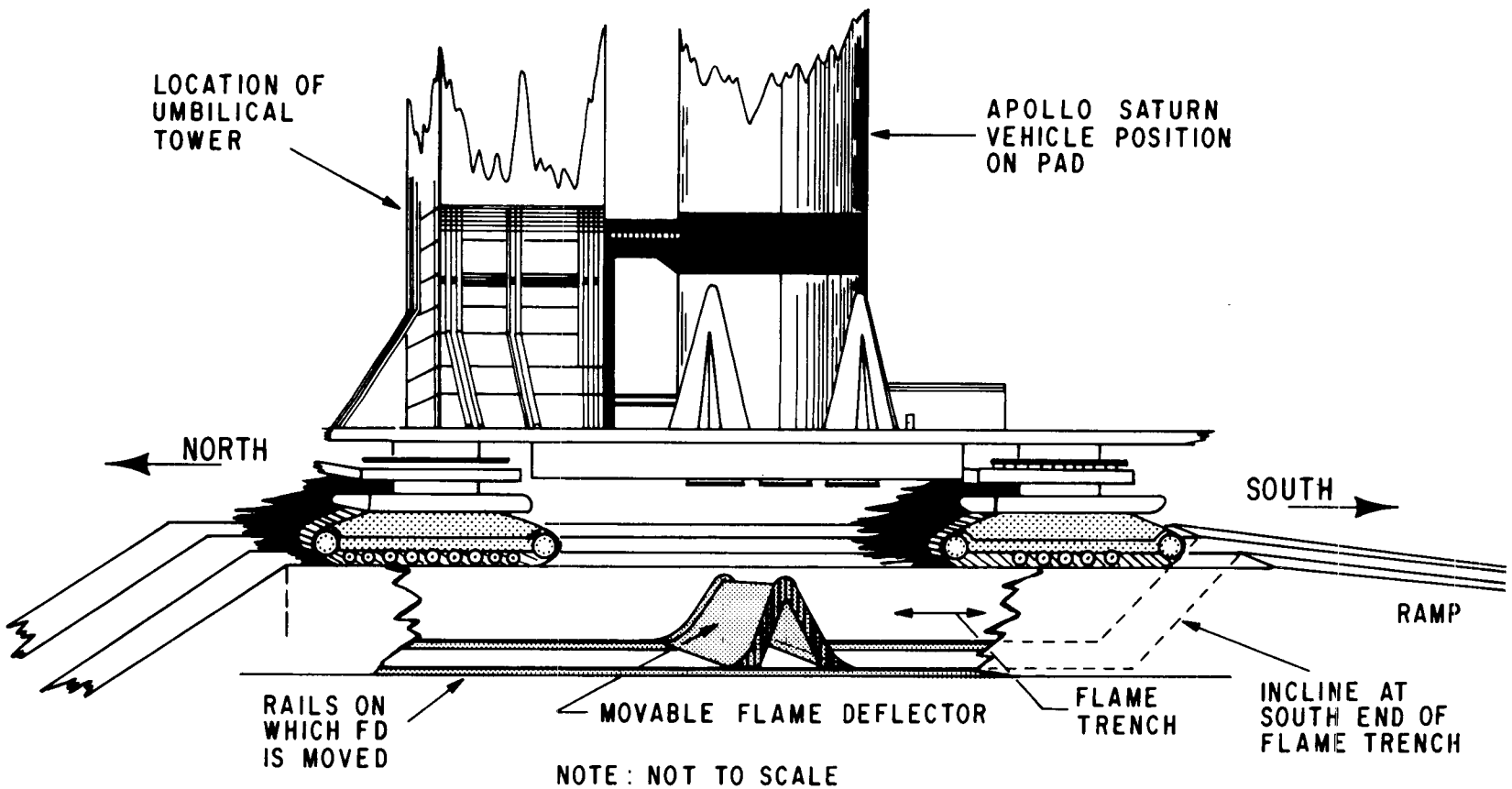

FIGURE 2. CUTAWAY VIEW OF LAUNCH COMPLEX 39A

engines produce about 1.34×10^{10} calories of heat per second. However, after evaporative cooling from the water spray during initial launch, only about 1.27×10^{10} calories of heat per second are emitted [4].

The exhaust cloud from the Apollo 16 launch was monitored photographically at two-second intervals to provide empirical data to evaluate cloud rise calculations from the Multilayer Diffusion Model.

The cloud rise and growth rate data were extracted from the sequential set of photographs by using scaling factors to account for the distance between the camera and the clouds, for the diameter of the top of the clouds and for time (Figures 3 and 4).

The predicted maximum cloud rise and the fitted curves of the observed rates of the bimodal cloud for Apollo 16 launch are shown in Figure 3. The greater rise rate of the right plume is due to deflection by the 21-degree inclination of the south end of the concrete flame trench. However, the two clouds eventually rise to an equal height and unite at the time they become stable with the ambient air.

b. Atmospheric Conditions at the Time of Launch of Apollo 16

Predictions of the concentration and movement of rocket motor effluents require inputs of several meteorological parameters varying in complexity from relatively straight forward ones such as potential temperature and wind velocity to rather complex ones such as standard deviations of the wind azimuth and elevation angles at all altitudes of interest. Selection of meteorological inputs begins with the assignment of layer boundaries based upon the vertical profiles of wind, temperature, and humidity within this volume.

The sources for meteorological information at Kennedy Space Center at the time of launch of Apollo 16 included the Jimsphere and radiosonde measurement systems, United States Air Force weather reconnainssance aircraft operating in the area, and the NASA 150-meter Ground Wind Tower on Merritt Island. Other sources of atmospheric data included synoptic weather maps and upper altitude atmospheric pressure and wind charts. Meteorologists from MSFC started analyses of meteorological data about two days before the launch of Apollo 16 to make preliminary plans for aircraft sampling profiles. These analyses continued up to the time of launch.

The atmospheric conditions in the vicinity of Kennedy Space Center Launch Complex 39 (LC39A) at the time of launch on April 16 were influenced primarily by dry stable air associated with an anti-cyclonic system centered off the east coast of Florida. Locally, there were only a few scattered cumulus clouds with bases at about two km. A

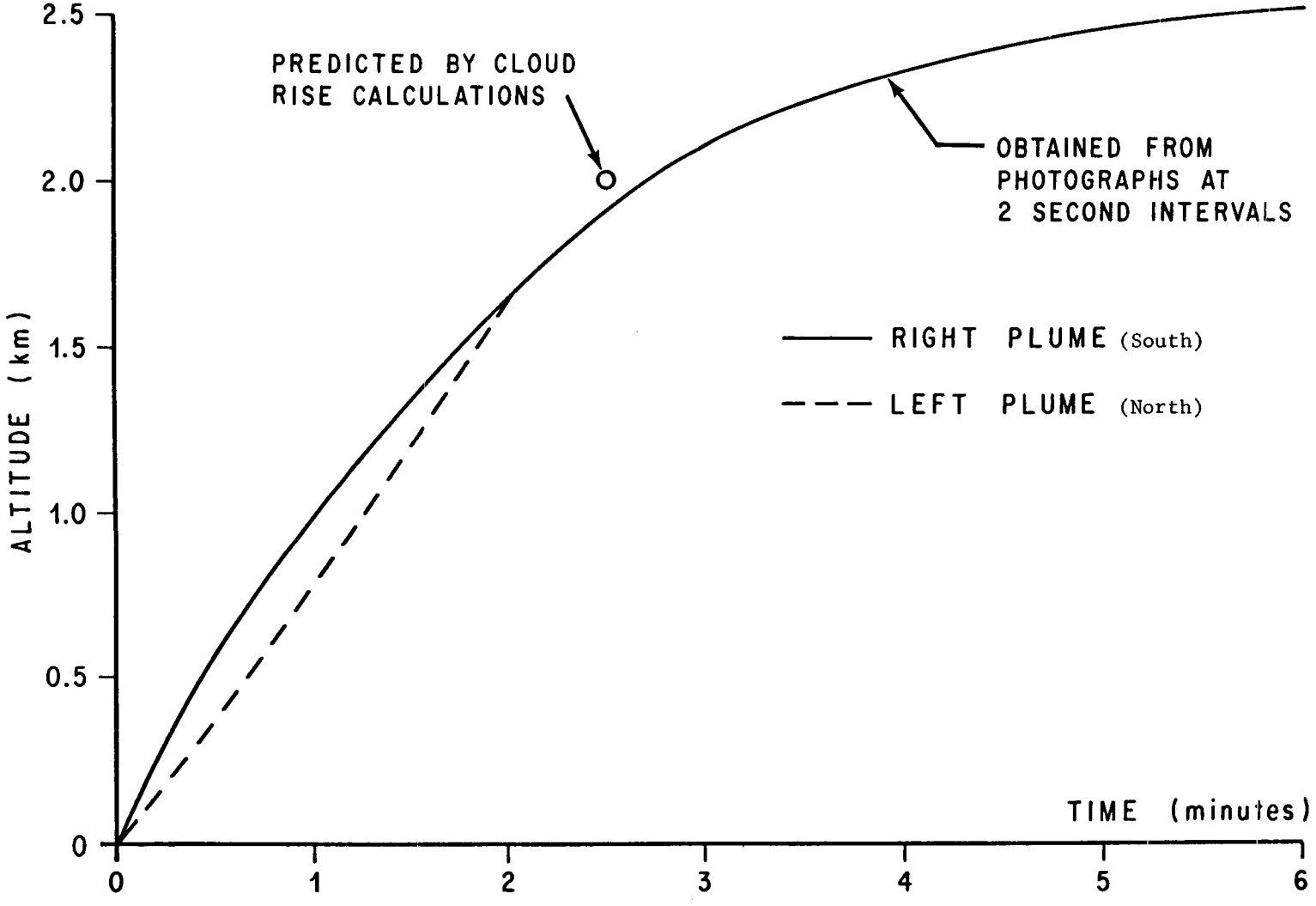

FIGURE 3. RISE RATE OF BIMODAL EXHAUST GROUND CLOUD FOR THE LAUNCH OF APOLLO 16 ON APRIL 16, 1972 (1754UT) AT KENNEDY SPACE CENTER, FLORIDA

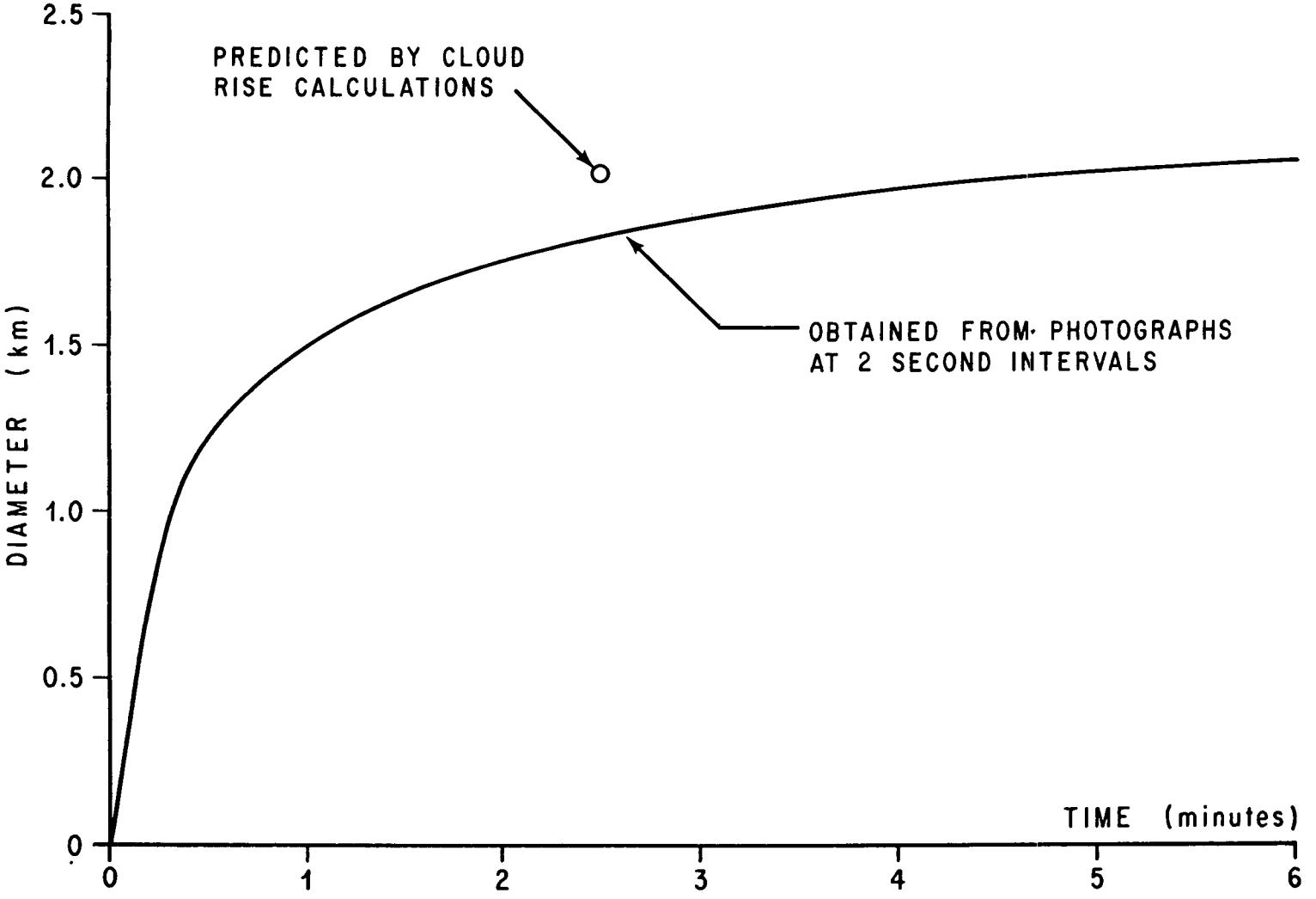

FIGURE 4. HORIZONTAL GROWTH OF GROUND CLOUD FOR THE LAUNCH OF APOLLO 16 ON APRIL 16, 1972 (1754UT) AT KENNEDY SPACE CENTER, FLORIDA

sea breeze had penetrated inland from the southeast across much of Cape Kennedy but had not reached as far as LC 39A. The wind was southwest at almost all altitudes from the surface to an altitude of 15 km (Figure 5). These persistent southwest winds were responsible for delaying and reducing the effect of the sea breeze. Wind speeds ranged from 5.0 m/sec at the surface to 26.1 m/sec at 11.9 km altitude. In addition to wind data, a crucial parameter influencing the altitude at which the ground exhaust cloud will stabilize is atmospheric stability. At the time of the Apollo 16 launch, a subsidence inversion existed over KSC, with a base of about 2000 m. This inversion had a profound effect on the ground exhaust cloud dynamics, and subsequently on the concentration of rocket engine effluents both at the ground cloud and ground surface levels.

The southwesterly wind pattern developed over Florida as a consequence of a low pressure trough moving eastward from the Mississippi Valley. As this trough shifted to the higher pressure existing over Florida, the pressure gradient increased through the troposphere resulting in fairly strong southwesterly winds. A rapidly moving cold front associated with the trough aloft was located over extreme northwest Florida at launch time, but the rain shower activity produced by this weather system was confined to the immediate vicinity of the front; therefore, the front had no direct effect on the local weather conditions. However, the influence of the weather system dominated the wind profile, and this factor was critical in making predictions of the ground exhaust cloud movement.

c. Meteorological and Source Inputs to the Model

Based on the vehicle used, in this case the Saturn V, and the meteorological conditions at the launch time, a set of values for meteorological and source model input parameters for the MSFC/NASA Multilayer Diffusion Model are defined. Time-lapse photographs are used primarily as an empirical standard comparison for the observed and predicted exhaust cloud rise and volume. A detailed list of the general input parameters required by the model is given in Appendix III. The specific values that were employed in the model to obtain the concentration-dosage mapping for the launch of the Saturn V vehicle in the Apollo 16 mission are given.

Calculations of the maximum height (z_m) of rise of the Apollo 16 engine exhaust ground cloud, to define the location and size of the source, were made using rawinsonde soundings at 6 hours 39 minutes before launch (1115 UT) to forecast and at 10 minutes after launch (1804 UT) to predict the environmental dispersion of these exhaust effluents. The values of the ambient temperature (T), the potential temperature gradient ($\partial\theta/\partial z$), and the mean wind speed ($\bar{u}$)

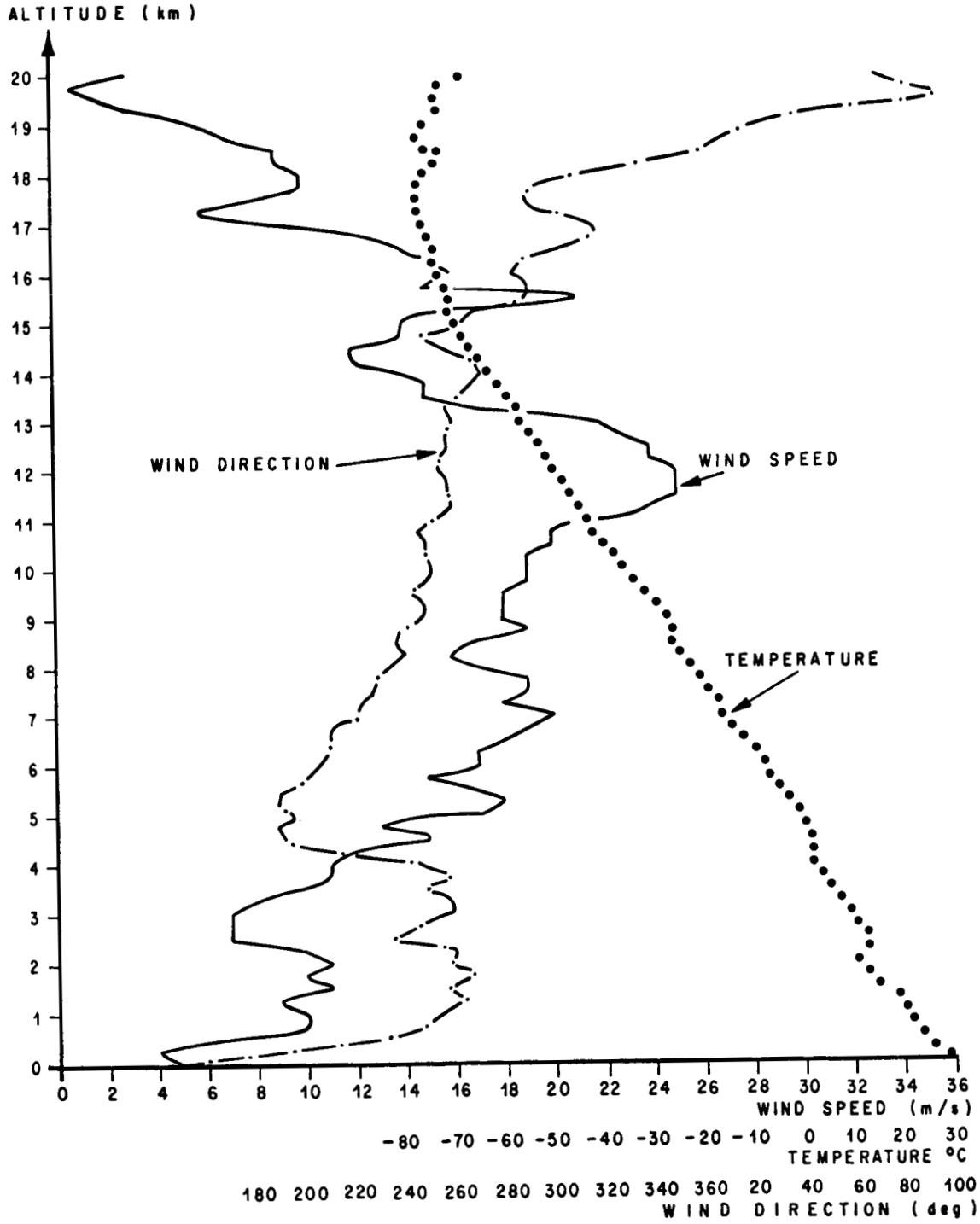

FIGURE 5. WIND AND TEMPERATURE PROFILES AT 10 MINUTES (1804 UT) AFTER THE LAUNCH OF APOLLO 16 ON APRIL 16, 1972

for these two soundings are given in Table III. This positive potential temperature gradient implies that a stable cloud rise relation is required (Equation A-2 or A-4). The relatively slow rise of the Saturn V ground Cloud dictates the use of the continuous cloud rise relation for the stable source. The initial vertical plume velocity (w_o), the initial radius (r_o), the entrainment coefficient (γ) (Table III) are required in the cloud rise calculation and are based on the characteristics of the Saturn V vehicle [4]. The maximum cloud rise calculated (Equation A-4) for the 1804 UT sounding is 2000 meters. This analytical prediction of the height in Figure 3 is compared to the observed cloud rise heights (solid curve) obtained using time-lapse photographs [5]. (While Figure 3 only gives a single analytically predicted cloud rise height, a predicted cloud rise curve can be analytically generated with Equation A-4.)

The height of cloud stabilization is then employed in the empirical prediction of the cloud diameter (Figure 4) based on the MSFC library of cloud growth observations. For comparison of the predicted with observed cloud diameter, the photographically observed cloud growth as a function of time was made.

The ground cloud became stable with the ambient air 150 seconds after launch and had a maximum height of about 2000 meters. At this time, the cloud contained 5.460×10^5 kilograms of the rocket engine effluents from approximately the first 43 seconds of engine operation. Calculations of the parts per million (ppm) of carbon monoxide in the stabilized cloud indicated about 130 ppm if uniform mixing occurred; however, in the application of the MSFC/NASA Multilayer Diffusion Model it is assumed the exhaust effluents in the cloud are Gaussian distributed in the plane of the horizon, resulting in a higher centerline concentration of carbon monoxide than the average value just given. Photographs of the cloud at 6.0 minutes after launch revealed that the ground cloud had assumed a shape modeled by oblate spheriodal (Figure 6). The major axes was 2000 meters in the x and y directions and the minor axis was 800 meters in the z direction (the x-axis is in the alongwind direction; y is in the crosswind direction; and z is in the vertical direction).

A detailed examination of the appropriate air temperature and dew point (Figure 7), and wind speed and direction (Figure 8) at the time of the launch of Apollo 16 indicated the atmosphere should be initially assumed to consist of nine layers. The top of seven of these layers are defined by the meteorological parameters indicated in these figures, and the other two layers are defined by cloud dimensions. Initially, the MSFC Multilayer Atmospheric Diffusion Model 1 (source extends vertically through the entire depth of the layer and vertical mixing is occurring) was applied to initiate the distributions. After stabilization of the ground exhaust cloud, it was assumed there was layer breakdown between the lowest six layers, and therefore turbulent mixing would occur in the first 2000 meters above the launch pad. Model 4 (full transition model for step-change in layer structure), with appropriate layer breakdown formulas was used to simulate

TABLE III.

INPUT PARAMETERS TO PLUME RISE FORMULAS

A. General			
1. Initial cloud radius at the surface	r_R	5m	
2. Air density	ρ	1190 g/m	
3. Entrainment constant	γ_c	0.5	
4. Specific heat of air at constant pressure	c_p	0.25 cal/g^{o}K	
5. Initial vertical plume velocity	w_o	488 m/sec	
B. Meteorological Regime			
		1115 UT	1804 UT
1. Ambient air temperature	T	294^{o}K	302^{o}K
2. Vertical potential temperature gradient	$\frac{\partial\theta}{\partial z}$	0.0055^{o}K	0.0028^{o}K/m
3. Mean wind speed	$\bar{u}$	7.0 m/sec	7.8 m/sec

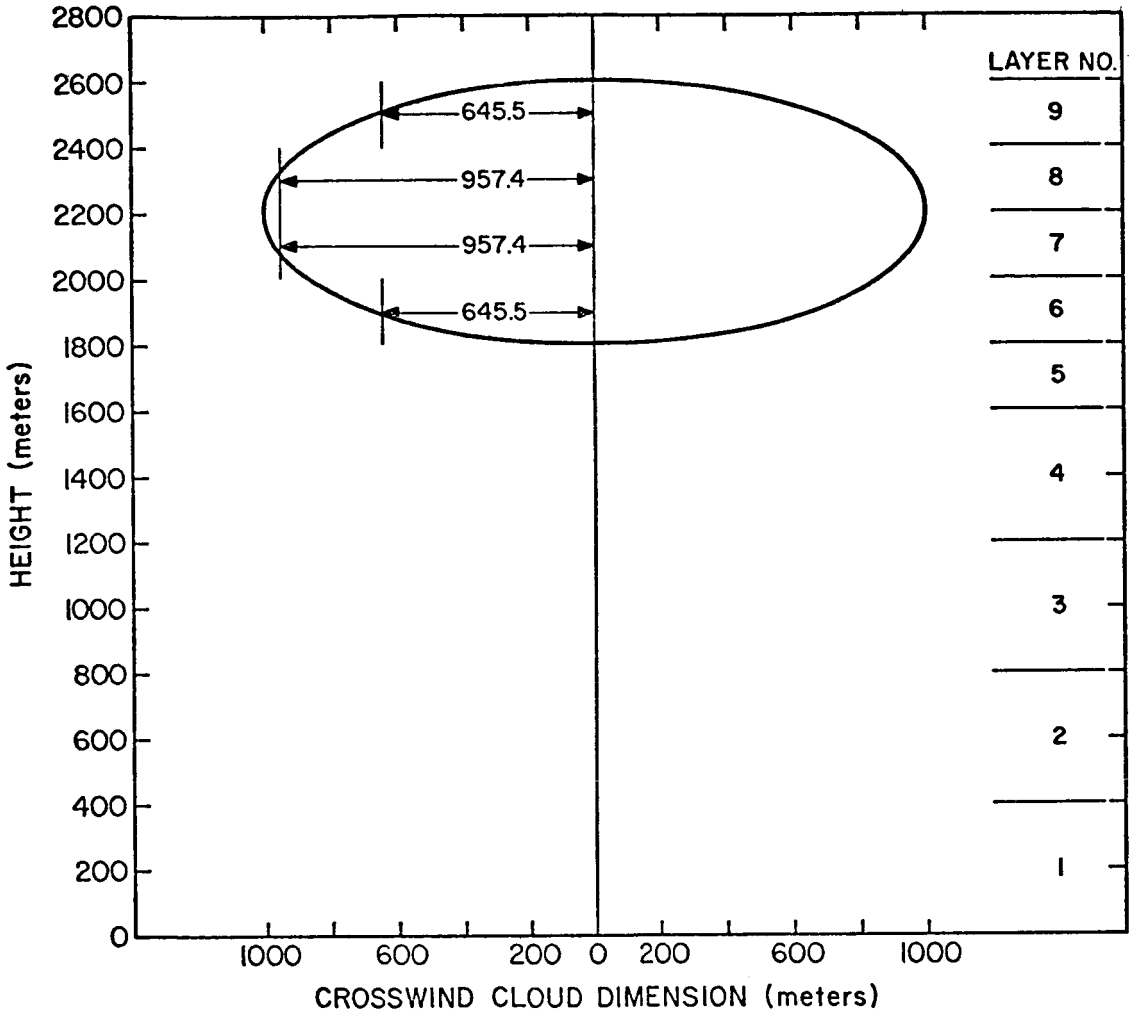

FIGURE 6. CROSSWIND AND VERTICAL CLOUD DIMENSIONS ASSIGNED TO THE GROUND CLOUD FORMED FROM THE LAUNCH OF APOLLO 16

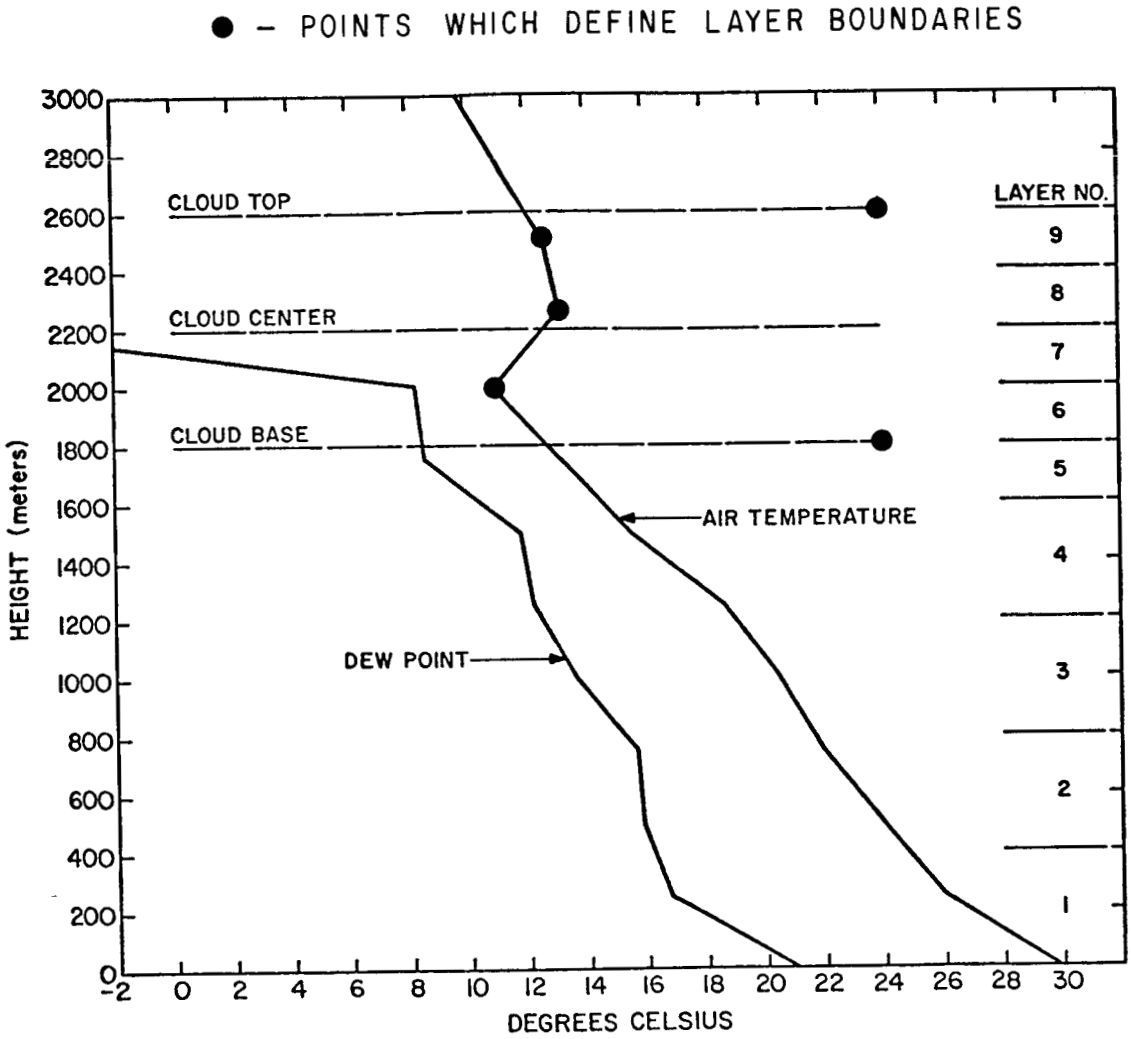

FIGURE 7. AIR TEMPERATURE AND DEW-POINT TEMPERATURE PROFILES FROM THE 1804 UT RAWINSONDE ON APRIL 16, 1972 AT CAPE KENNEDY

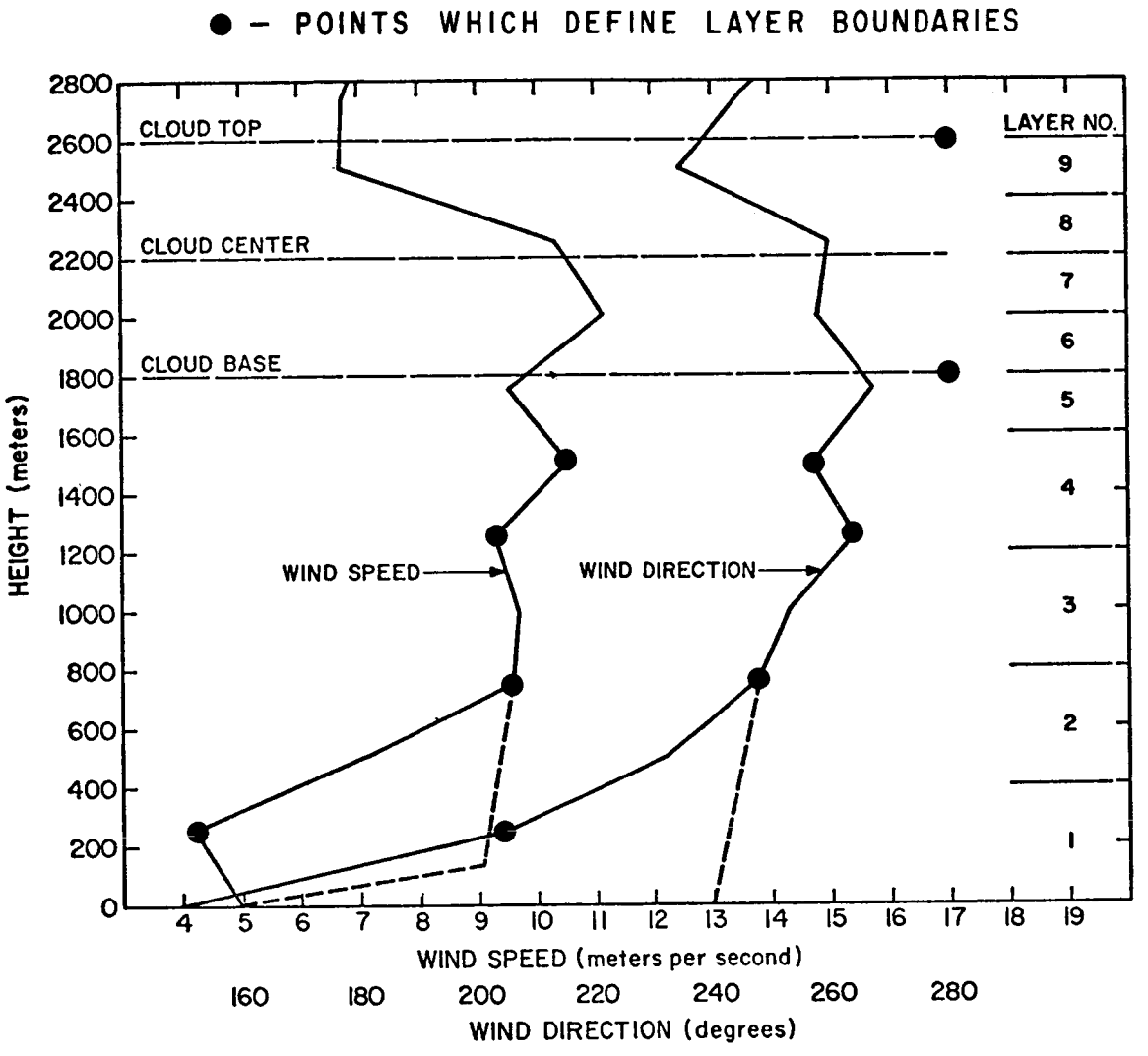

FIGURE 8. WIND SPEED AND DIRECTION PROFILES FROM THE 1804 UT RAWINSONDE ON APRIL 16, 1972 AT CAPE KENNEDY (SOLID LINES). DASHED LINES REPRESENT ADJUSTED PROFILES BASED ON INFORMATION FROM THE 150-METER GROUND WIND TOWER

the effects of this turbulent mixing of the six lowest layers. Between altitudes of 2000 meters and 4000 meters (altitude of the next inversion layer), Model 3 (vertical extend of the source is less than the depth of the layer) was assumed. This resulted in trapping of all engine effluents of the ground exhaust cloud that were above an altitude of 2000 meters within the altitude region 2000 to 4000 m. The portion of the ground exhaust cloud contained between altitudes of 1800 and 2000 meters was assumed to mix and diffuse downward to the ground.

Source and meteorological input parameters for the MSFC/ NASA Multilayer Diffusion Model are defined in Appendix III (Tables A-I and A-III). The values of the meteorological input in Table IV are for all nine layers prior to the breakdown of the layers. Values for the source dimensions and source strengths in a respective layer were obtained relative to the stabilized ground cloud (Figure 6) utilizing the relations in Appendix III (Equation A-39, A-40, and A-41). The resulting source parameter for the launch of Apollo 16 are given in Table V. These meteorological and source input parameters (Tables IV and V) are the basis of the effluent dispersion results for the launch of Apollo 16 that were obtained with the NASA/MSFC Multilayer Diffusion Model.

d. Predictions of the Concentration Contours from Exhaust Effluents for Apollo 16 by the NASA/MSFC Multilayer Diffusion Model

The following predictions for the dispersion of the Saturn V exhaust effluents from the Apollo 16 mission will focus on the dispersion of carbon monoxide and carbon dioxide because these are the only two constituents that are potentially toxic and have a potential impact on the environment air quality in the troposphere. Carbon monoxide is selected as the trace gas in the isopleths and centerline concentration profiles that are discussed because the concentrations of carbon monoxide are 2.4 times stronger than those of carbon dioxide and because the toxicity levels for carbon monoxide are much less than those for carbon dioxide (Appendix IV); that is, if there is not an environmental hazard from carbon monoxide during the launch of a Saturn V vehicle, then it can be assumed that the other constituents in the exhaust effluents will not afford an environmental hazard.

To ascertain the surface concentrations of carbon monoxide a nine layer atmosphere structure (Figures 7 and 8) was employed, based on the atmospheric thermodynamic and kinematic soundings at launch time, initially in Model 1 of the NASA/MSFC Multilayer Diffusion Model (as discussed in the last section) and run for one second. Then Model 4 was invoked to merge the first six layers. The top of this new surface layer was dictated by the temperature inversion at 2 kilometers. The

TABLE IV.

METEOROLOGICAL MODEL INPUTS FOR THE NINE LAYERS

Parameter	Units	Layer								
		1	2	3	4	5	6	7	8	9
$\bar{u}_R$	m sec^{-1}	5.24								
$\bar{u}_{BK}$	m sec^{-1}	5.0	9.3	9.6	9.4	10.1	9.9	11.1	10.5	8.1
$\bar{u}_{TK}$	m sec^{-1}	9.3	9.6	9.4	10.1	9.9	11.1	10.5	8.1	6.7
θ_{BK}	^oK	301.0	301.9	301.7	301.8	301.9	301.8	302.1	305.8	308.3
θ_{TK}	^oK	301.9	301.7	301.8	301.9	301.8	302.1	305.8	308.3	309.5
$\sigma_{AR}\{\tau_{oK}\}$	deg	8.66								
$\sigma_{ABK}\{\tau_{oK}\}$	deg	9.08	4.92	4.54	4.34	5.19	4.14	4.09	2.0	1.0
$\sigma_{ATK}\{\tau_{oK}\}$	deg	4.92	4.54	4.34	4.19	4.14	4.09	2.0	1.0	1.0
τ_{oK}	sec	600	600	600	600	600	600	600	600	600
α_K		1	1	1	1	1	1	1	1	1

TABLE V.

SOURCE INPUTS FOR STABILIZED CLOUD

Parameter	Units	Layer								
		1	2	3	4	5	6	7	8	9
z_R	m	3								
z_{BK}	m	2	400	800	1200	1600	1800	2000	2200	2400
z_{TK}	m	400	800	1200	1600	1800	2000	2200	2400	2600
T_K	sec	180	180	180	180	180	180	180	180	180
$\sigma_{yo}\{K\}$	m	0	0	0	0	0	300.2	445.3	445.3	300.2
$\sigma_{xo}\{K\}$	m	0	0	0	0	0	300.2	445.3	445.3	300.2
Q_K	ppm m^{-1}	0	0	0	0	0	1.694×10^8	4.411×10^8	4.539×10^8	2.118×10^8

resulting isopleths are shown in Figure 9. These isopleths represent the spatial mapping at the bottom of the original six layers. This spatial selection represents the significant locations (defined by meteorological conditions) required in an environmental inventory of the impact of the rocket exhaust effluents. Of obvious importance are the surface (2 meter level) isopleths, which reveal that the maximum concentration of carbon monoxide was less than 2 ppm from the launch of Apollo 16. This is well below the public exposure level of 25 ppm in an one-hour period recommended by the Environmental Protection Agency (Appendix IV, Table A-III). The maximum centerline downwind concentrations of CO and CO_2 at the bottom of the layers between the source center (2.2 kilometers) and the surface are shown in Table VI. Turbulent mixing and diffusion processes diluted the constituents rapidly, as can be observed from the small quantities that reached ground level. To convert concentrations of CO (as indicated by the isopleths in Figure 9) to CO_2, it is necessary to multiply by a conversion factor of .4203. The factor was determined from the following relationship:

$$\text{ppm (CO)} \times \frac{28.8\%\ CO_2}{43.6\%\ CO} \times \frac{\text{molecular WT of CO}}{\text{molecular WT of } CO_2} = \text{ppm } (CO_2) \quad (4)$$

The 28.8% CO_2 and 43.6% CO values in the above equation represent the estimated percentage by weight of these Saturn engine exhaust constituents after reaction with the atmosphere.

Four downwind maximum centerline concentrations of carbon monoxide were calculated, ranging in alitutde from 2.2 kilometers, which was the center of the stabilized ground cloud, to 17.5 kilometers. The upper three altitudes (3.5 km, 8.5 km, and 17.5 km) were selected to correspond to the alitutdes at which Air Force aircraft obtained samples. The ground cloud (2.2 km) was treated as an oblate spheroid (this is the original ground cloud) utilizing Model 3. In the remaining three levels, the source is the plume cloud of uniform cylindrical concentration. The cylinders are assumed to have a height of 1.0 kilometer and a diameter of 400 meters after a cloud stabilization time of 30 seconds (Figure 10). The height of these layers affect the concentration because Model 1, which assumes a uniform vertical concentration, is used. The concentrations downwind are given in Figure 11 for these four altitudes. This figure shows that the downwind concentrations at 8.5 kilometers and 17.5 kilometers altitude are greater than those at 3.5 kilometers beyond a downwind distance of 20 kilometers; showing clearly the support transport effect of the isothermal layer at an altitude of about 4.0 kilometers. The reason that the concentrations decreases as a function of increasing altitude is that the vehicle gains speed as its altitude increases and therefore spends less time in each layer as it ascends.

TABLE VI. GROUND CLOUD DATA

Maximum Centerline Concentrations of CO and CO_2 for the AS-511 Ground Cloud in ppm

Downwind Distance (meters)	Altitude (meters) 2.0		400		800		1200		1600		1800		2200*	
	CO	CO_2	CO	CO_2	CO	CO_2	CO	CO_2	CO	CO_2	CO	CO_2	CO	CO_2
2000	0	0	0	0	0	0	$.143 \times 10^{-5}$	$.601 \times 10^{-6}$	$.444 \times 10^{1}$	$.186 \times 10^{1}$	$.959 \times 10^{2}$	$.403 \times 10^{2}$	$.295 \times 10^{3}$	$.124 \times 10^{3}$**
4000	0	0	0	0	$.423 \times 10^{-4}$	$.178 \times 10^{-4}$	.181	$.760 \times 10^{-1}$	$.200 \times 10^{2}$	$.841 \times 10^{1}$	$.601 \times 10^{2}$	$.253 \times 10^{2}$	$.222 \times 10^{3}$	$.933 \times 10^{2}$
6000	0	0	$.157 \times 10^{-3}$	$.660 \times 10^{-4}$	$.402 \times 10^{-1}$	$.169 \times 10^{-1}$	$.199 \times 10^{1}$	.838	$.199 \times 10^{2}$	$.837 \times 10^{1}$	$.352 \times 10^{2}$	$.148 \times 10^{2}$	$.170 \times 10^{3}$	$.716 \times 10^{2}$
8000	$.505 \times 10^{-3}$	$.212 \times 10^{-3}$	$.156 \times 10^{-1}$	$.656 \times 10^{-2}$	.387	.163	$.380 \times 10^{1}$	$.159 \times 10^{1}$	$.149 \times 10^{2}$	$.625 \times 10^{1}$	$.209 \times 10^{2}$	$.878 \times 10^{1}$	$.133 \times 10^{3}$	$.561 \times 10^{2}$
10000	$.158 \times 10^{-1}$	$.664 \times 10^{-2}$	.117	$.492 \times 10^{-1}$	.950	.399	$.424 \times 10^{1}$	$.178 \times 10^{1}$	$.104 \times 10^{2}$	$.437 \times 10^{1}$	$.130 \times 10^{2}$	$.548 \times 10^{1}$	$.107 \times 10^{3}$	$.448 \times 10^{2}$
11000	$.438 \times 10^{-1}$	$.184 \times 10^{-1}$	.207	$.870 \times 10^{-1}$	$.118 \times 10^{1}$	.496	$.411 \times 10^{1}$	$.173 \times 10^{1}$	$.869 \times 10^{1}$	$.365 \times 10^{1}$	$.105 \times 10^{2}$	$.441 \times 10^{1}$	$.958 \times 10^{2}$	$.403 \times 10^{2}$
12000	$.926 \times 10^{-1}$	$.389 \times 10^{-1}$	.312	.131	$.134 \times 10^{1}$	.566	$.386 \times 10^{1}$	$.162 \times 10^{1}$	$.728 \times 10^{1}$	$.306 \times 10^{1}$	.853 x 10^{1}	$.358 \times 10^{1}$	$.866 \times 10^{2}$	$.364 \times 10^{2}$
13000	.161	$.677 \times 10^{-1}$	.418	.176	$.144 \times 10^{1}$	.607	$.358 \times 10^{1}$	$.149 \times 10^{1}$	$.613 \times 10^{1}$	$.257 \times 10^{1}$	.702 x 10^{1}	$.295 \times 10^{1}$	$.785 \times 10^{2}$	$.330 \times 10^{2}$
14000	.244	.103	.518	.218	$.149 \times 10^{1}$	.625	$.324 \times 10^{1}$	$.136 \times 10^{1}$	$.518 \times 10^{1}$	$.217 \times 10^{1}$	.583 x 10^{1}	$.245 \times 10^{1}$	$.715 \times 10^{2}$	$.301 \times 10^{2}$
15000	.334	.140	.605	.254	$.148 \times 10^{1}$	.622	$.293 \times 10^{1}$	$.123 \times 10^{1}$	$.441 \times 10^{1}$	$.185 \times 10^{1}$	.489 x 10^{1}	$.206 \times 10^{1}$	$.654 \times 10^{2}$	$.275 \times 10^{2}$
20000	.670	.282	.815	.343	$.121 \times 10^{1}$	.508	$.172 \times 10^{1}$	.723	$.216 \times 10^{1}$	.906	.228 x 10^{1}	.960	$.437 \times 10^{2}$	$.184 \times 10^{2}$
25000	.717	.301	.769	.323	.904	.380	$.107 \times 10^{1}$	.450	$.121 \times 10^{1}$	.508	.125 x 10^{1}	.525	$.311 \times 10^{2}$	$.131 \times 10^{2}$
30000	.624	.262	.639	.269	.680	.286	.731	.307	.772	.324	.784	.330	$.233 \times 10^{2}$	$.980 \times 10^{1}$
40000	.404	.170	.405	.170	.407	.171	.411	.173	.413	.174	.414	.174	$.149 \times 10^{2}$	$.626 \times 10^{1}$
50000	.266	.112	.266	.112	.266	.111	.266	.112	.266	.112	.266	.111	$.111 \times 10^{2}$	$.466 \times 10^{1}$
60000	.187	$.786 \times 10^{-1}$	.187	$.786 \times 10^{-1}$	.187	$.786 \times 10^{-1}$	.186	$.784 \times 10^{-1}$	.187	$.784 \times 10^{-1}$	.186	$.784 \times 10^{-1}$	$.910 \times 10^{1}$	$.382 \times 10^{1}$
70000	.138	$.580 \times 10^{-1}$	.138	$.580 \times 10^{-1}$	.138	$.580 \times 10^{-1}$	.138	$.580 \times 10^{-1}$	.138	$.580 \times 10^{-1}$	.138	$.582 \times 10^{-1}$	$.780 \times 10^{1}$	$.327 \times 10^{1}$
80000	.106	$.446 \times 10^{-1}$	.106	$.446 \times 10^{-1}$	.106	$.446 \times 10^{-1}$	.106	$.446 \times 10^{-1}$	.106	$.446 \times 10^{-1}$	.106	$.446 \times 10^{-1}$	$.690 \times 10^{1}$	$.290 \times 10^{1}$
90000	$.842 \times 10^{-1}$	$.354 \times 10^{-1}$	$.842 \times 10^{-1}$	$.354 \times 10^{-1}$	$.842 \times 10^{-1}$	$.354 \times 10^{-1}$	$.842 \times 10^{-1}$	$.354 \times 10^{-1}$	$.843 \times 10^{-1}$	$.354 \times 10^{-1}$	$.843 \times 10^{-1}$	$.354 \times 10^{-1}$	$.610 \times 10^{1}$	$.256 \times 10^{1}$
100000	$.684 \times 10^{-1}$	$.287 \times 10^{-1}$	$.684 \times 10^{-1}$	$.287 \times 10^{-1}$	$.684 \times 10^{-1}$	$.287 \times 10^{-1}$	$.684 \times 10^{-1}$	$.287 \times 10^{-1}$	$.684 \times 10^{-1}$	$.287 \times 10^{-1}$	$.684 \times 10^{-1}$	$.288 \times 10^{-1}$	$.550 \times 10^{1}$	$.231 \times 10^{1}$

*Height at center of stabilized cloud

**Concentrations are high at center of cloud because of gaussian assumptions

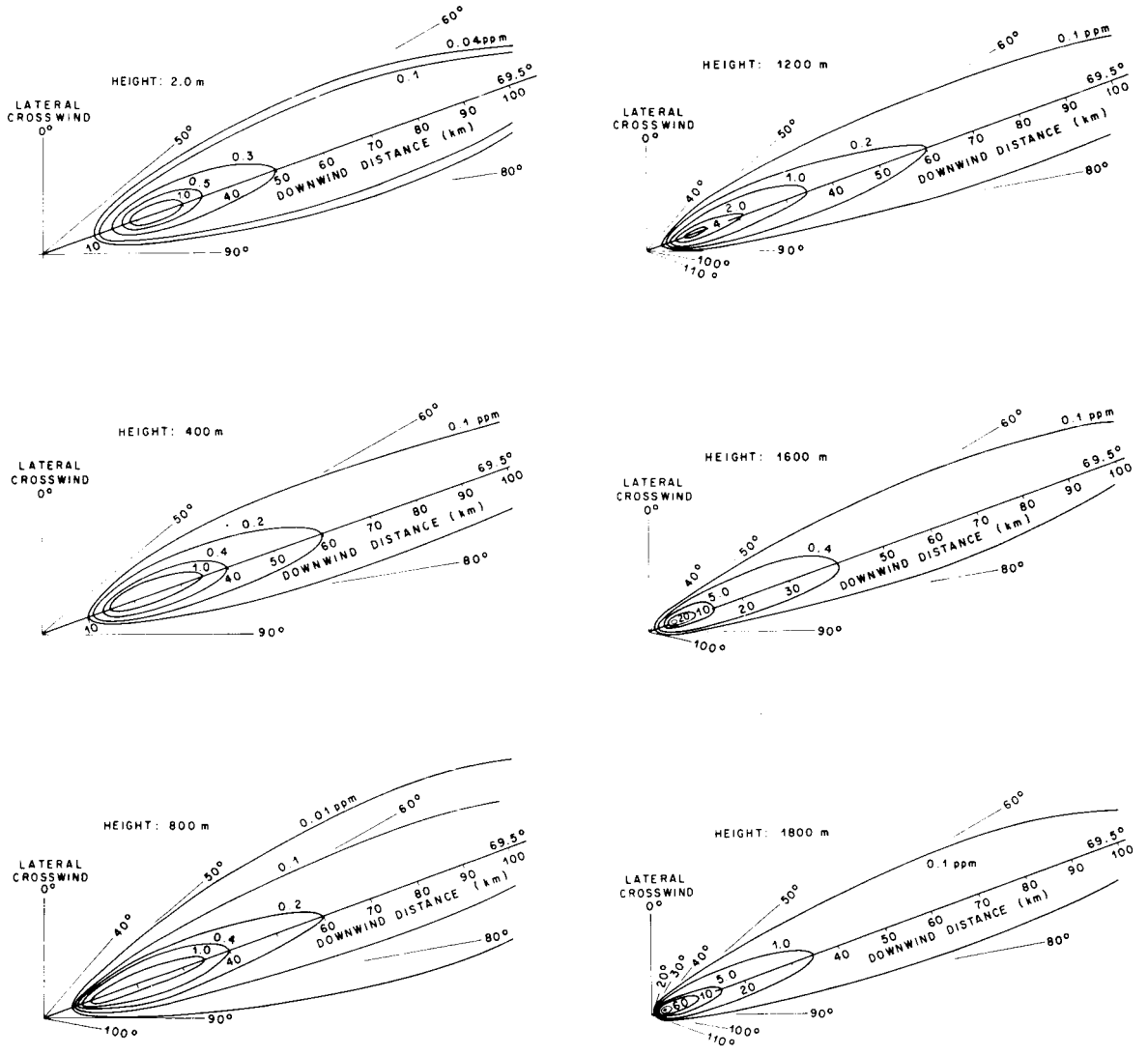

FIGURE 9. ISOPLETHS OF CARBON MONOXIDE FOR THE GROUND CLOUD PEAK CONCENTRATIONS (ppm) (CONCENTRATIONS GREATER THAN 0.5 HAVE BEEN ROUNDED OFF TO THE NEAREST INTEGER)

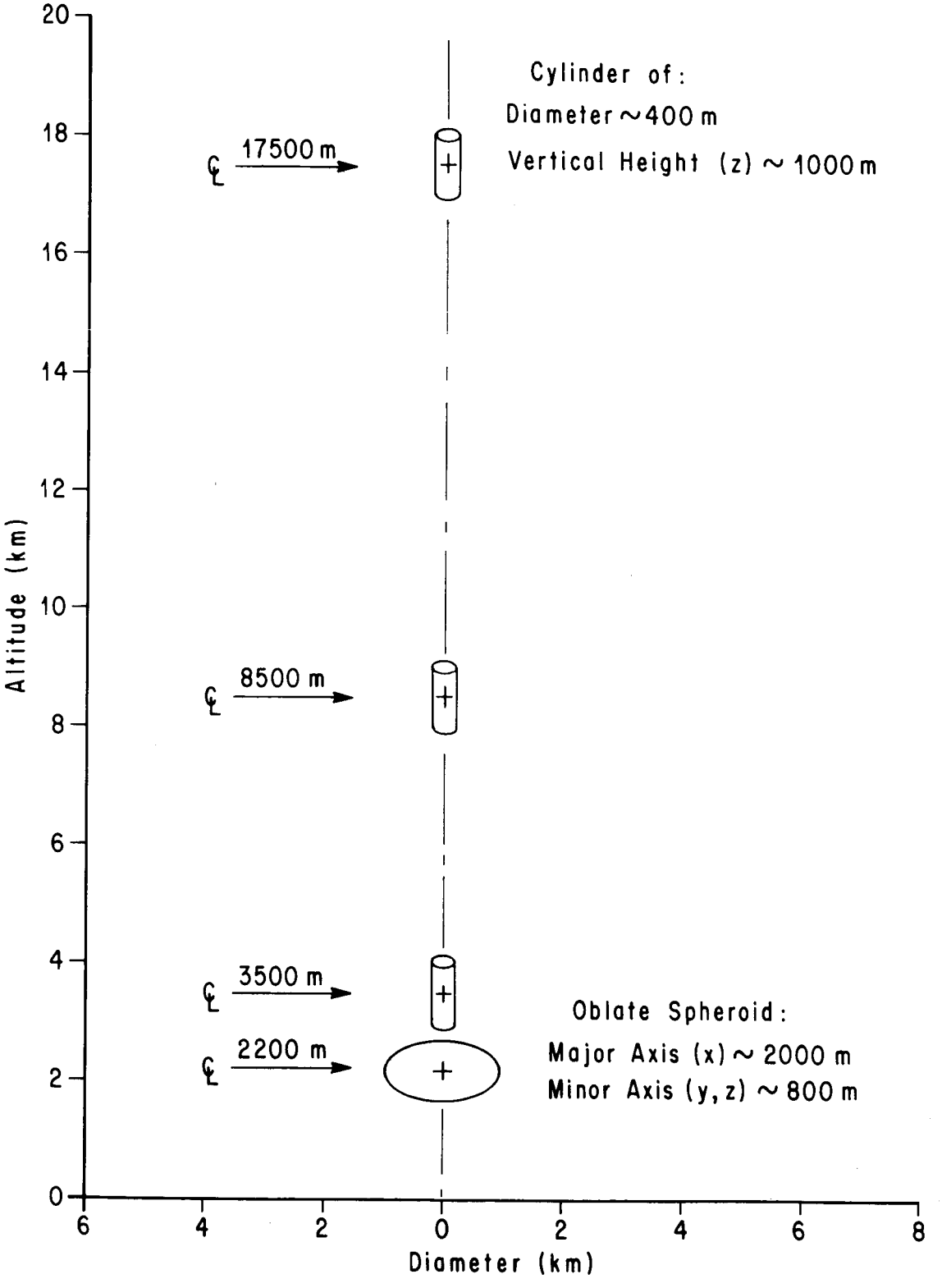

FIGURE 10. CLOUD MODEL USED TO OBTAIN UPPER AIR CENTERLINE CONCENTRATIONS

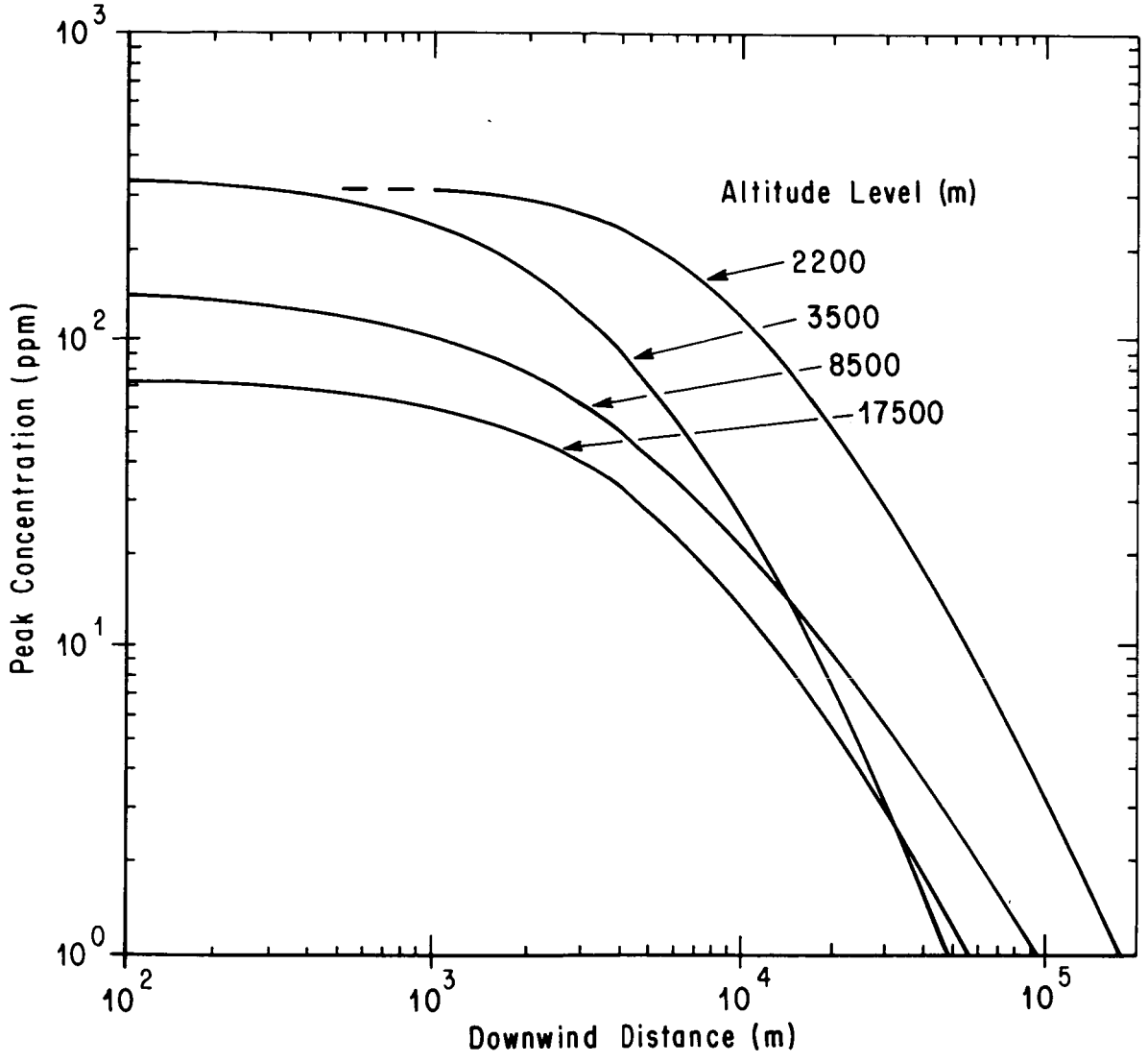

FIGURE 11. UPPER ATMOSPHERE PEAK CENTERLINE CONCENTRATIONS OF CARBON MONOXIDE

In summary, these calculations indicated maximum ground level concentrations of CO of less than 2 ppm for the Apollo 16 launch, well below the 25 ppm maximum allowable one-hour concentrations allowed by the Environmental Protection Agency. The maximum calculated concentration of CO in the ground exhaust cloud at an altitude of 2200 meters was 295 ppm, rapidly diminishing to 23 ppm by turbulent mixing and diffusion processes at a downwind distance of about 30 km.

SECTION IV. PREDICTIONS OF THE DISPERSIVE TRANSPORT OF SCOUT-ALGOL III MOTOR EXHAUST EFFLUENTS IN THE TROPOSPHERE (AUGUST 13, 1972)

Concentration mappings of the exhaust effluents from the launch of the Scout-Algol III vehicle at 1510 Universal Time (UT) (1110 EDT) from Wallops Island, Virginia, obtained from the NASA/MSFC Multilayer Diffusion Model are presented in this section. The calculation of the exhaust effluent dispersion presented in this report are limited to altitudes below 500 meters because the exhaust effluents released by the Scout vehicle are relatively small; therefore, only the ground cloud affords a sufficiently intensity source of effluents for a meaningful analysis at the surface. In contrast to the Saturn V exhaust effluents, the Scout exhaust effluents contain more potentially toxic constituents and, obviously, because of the size of the Scout, the concentrations of these efflunets are much less.

As it was illustrated in the last section, the two important parametric inputs in the MSFC/NASA Multilayer Diffusion Model are the vehicle fuel properties and the meteorological conditions; these Scout-Algol input parameters will be discussed as an introduction to the actual model parameters employed and the predictions obtained.

a. Algol III Motor Exhaust Effluents

It has been established theoretically and from observations that low altitude clouds of motor exhaust and entrained gases are formed during the launch of the Algol III booster. In the case of the Scout-Algol III vehicle, these clouds regularly rise and stabilize at an altitude of about 400 meters (based on empirical observations) depending upon meteorological conditions. The motor exhaust effluents contained in this cloud are produced during the period from rocket ignition to the time that it ascends to the altitude at which the exhaust ground cloud stabilizes. For a cloud stabilization altitude of 400 meters, the ground cloud contains the exhaust effluents produced during the first eight seconds of motor ignition, or about 1592 kg of material (Table VII). The composition of these solid rocket motor exhaust effluents consists primarily (98.3 percent, see Table VIII) of, in order of descending concentration, alumina (Al_2O_3), carbon monoxide (CO), hydrogen chloride (HCl), nitrogen (N_2), water vapor (H_2O), hydrogen (H_2), and carbon dioxide (CO_2). Four are potentially toxic (see Appendix IV). The stabilized ground cloud from the Scout-Algol III contained about 511 kg of alumina, 436 kg of carbon monoxide, 328 kg of hydrogen chloride, and only 33 kg of carbon dioxide.

The rocket plume from the Scout-Algol III before lift-off impinges on a steel plate surrounded by concrete in contrast to the flame trench with water that is employed for Saturn launches. The resulting

TABLE VII.

EXHAUST MATERIALS EMITTED AS A FUNCTION OF ALTITUDE FROM THE ALGOL III MOTOR

Range Time at Top of Layer (Seconds)	Altitude Range (meters)	Exhaust Material Emitted in Layer (kilograms)	Total Exhaust Material Emitted Thru Layer (kilograms)
1.000	0.00 - 5.49	208	208
3.049	5.49 - 57.30	432	640
5.097	57.30 - 159.41	411	1051
7.146	159.41 - 307.24	385	1436
9.195	307.24 - 497.13	374	1810
11.244	497.13 - 728.78	372	2182
13.292	728.78 - 1002.18	371	2552
15.341	1002.18 - 1318.26	370	2923
17.390	1318.26 - 1677.62	359	3282
19.439	1677.62 - 2079.04	359	3641
21.487	2079.04 - 2521.61	359	4000
23.536	2521.61 - 3003.19	350	4350
25.585	3003.19 - 3523.18	346	4696
35.829	3523.18 - 6693.10	1803	6499
46.072	6693.10 - 10933.48	1999	8498
56.316	10933.48 - 16600.02	2082	10580
66.560	16600.02 - 24002.60	1639	12219
78.852	24002.60 - 33440.52	541	12760

TABLE VIII.

FUEL PROPERTIES OF THE SCOUT-ALGOL III FIRST-STAGE MOTOR

Exhaust Products at Exit (percent by weight):		
Alundum	- Al_2O_3**	32.1
Carbon Monoxide	- CO**	27.4
Hydrogen Chloride	- HCl**	20.6
Nitrogen	- N_2	7.2
Water Vapor	- H_2O	6.4
Hydrogen	- H_2	2.5
Carbon Dioxide	- CO_2**	2.1
	Other	1.7

Fuel Expenditure Rate (g sec^{-1})	1.9414×10^5*
Fuel Heat Content (cal g^{-1})	979.4
Total Burn Time (sec)	78

*Exact values are given in Table VII - this value is the average over the initial 13.3 seconds of ascent.
**Potentially toxic (see Appendix IV)

Scout-Algol III plume is cylindrically symmetrical rather than a bimodal Saturn V plume. Another difference between the Scout and Saturn vehicle launches is that the Scout lift-off is milliseconds after ignition, rather than the 7 seconds associated with the Saturn. As a result of these factors, the vast amount of entrained water found in the Saturn V ground cloud is not present in the Scout ground cloud.

The exhaust cloud from the Scout-Algol III launch was monitored photographically at five-second intervals to provide empirical data to evaluate cloud rise calculations from the Multilayer Diffusion Model. Two cameras were employed in an orthogonal configuration west and south of the launch area, pointing toward the launch area.

The cloud rise and growth rate data were extracted from the sequential set of photographs by using scaling factors to account for the distance between the camera and the clouds, for the diameter of the top of the clouds and for time.

b. Atmospheric Conditions at the Time of Launch of the Scout-Algol III

Predictions of the concentration and movement of rocket motor effluents require inputs of several meteorological parameters varying in complexity from relatively straight forward ones such as potential temperature and wind velocity to rather complex ones such as standard deviations of the wind azimuth and elevation angles at all altitudes of interest. Selection of meteorological inputs begins with the assignment of layer boundaries based upon the vertical profiles of wind, temperature, and humidity within this volume.

The sources for meteorological information at Wallops Island at the time launch of the Scout included rawinsonde measurements, and the two NASA 76-meter Ground Wind Towers. Other sources of atmospheric data included synoptic weather maps and upper altitude atmospheric pressure and wind charts. Meteorologists from MSFC started analyses of meteorological data about two days before the launch of the Scout-Algol III vehicle to make preliminary plans for aircraft sampling profiles. These analyses continued up to the time of launch.

The atmospheric conditions in the vicinity of the Wallops Island launch site at 1510 UT on August 13, 1972 were dominated by partially cloudy skies, light winds and a surface temperature of 25°C. No strong surface pressure systems were in the immediate area, although a weak cold front over northern Virginia was moving toward the launch site. Precipitation was not evident in the Wallops area at launch time and cloud layers were primarily high (4km to 6km). This frontal system was in conjunction with a short wave of low pressure aloft moving through the long wave pattern established over the east coast of the United States

and the western Atlantic Ocean. The surface wind was southerly at 3.9 m/sec. The rawinsonde sounding (Figures 12 & 13) taken 40 minutes prior to launch (1430 UT), indicated a baroclinic spiraling of the wind direction such that at 2 kilometers the wind direction had shifted to a westerly direction. The wind speed, however, decreased with altitude to a near calm at the base of the elevated inversion (1.2 kilometers); at the top of this inversion (1.5 kilometers) it increased with altitude to about 3 m/sec at 2.6 kilometers. The temperature soundings shows a nearly dry adiabatic lapse rate from the surface to an altitude of 262 meters and again above 805 meters. The layer between 262 meters and 805 meters was a stable layer which is critical to the prediction of the top of the surface mixing layer.

c. Meteorological and Source Inputs to the Model

Based on the vehicle used, in this case the Scout-Algol III, and the meteorological conditions at the launch time, a set of values for meteorological and source model input parameters for the MSFC/NASA Multilayer Diffusion Model were defined. Time-lapse photographs were used primarily as an empirical comparison between predicted and observed exhaust cloud rise and volume. A detailed list of the general input parameters required by the model is given in Appendix III. The specific values that were employed in the model to obtain the concentration mappings for the launch of the Scout-Algol III vehicle are given.

Calculations of the maximum height (z_m) of rise of the Scout motor exhaust ground cloud, to define the location and size of the source, were made using rawinsonde soundings forty (40) minutes before launch (1430 UT) to predict the environmental dispersion of these exhaust effluents. The values of the ambient temperature (T), and the potential temperature gradient ($\partial\theta/\partial z$) for this sounding is given in Table IX. This positive potential temperature gradient implies that a stable cloud rise relation is required (Equation A-2 or A-4). Because of the almost instantaneous rise of the solid fuel rockets, the instantaneous rise of the solid fuel rockets, the instantaneous cloud rise relation (spherical entrainment) for a stable environment (Equation A-2) is required to describe the Scout's ground cloud rise. The initial radius at the surface (r_R) and the entrainment coefficient (8) in Table IX are required in the cloud rise calculations and are based on characteristics of the Scout-Algol III vehicle. Based on limited experience in predicting cloud rise from solid rocket motor launches at Vandenberg Air Force Base, this assumption appears to be justified. The time required for the cloud to reach the stabilization height is given by the expression

$$t = \frac{\pi}{\left(\frac{g}{T}\frac{\partial\theta}{\partial z}\right)^{\frac{1}{2}}} \qquad (5)$$

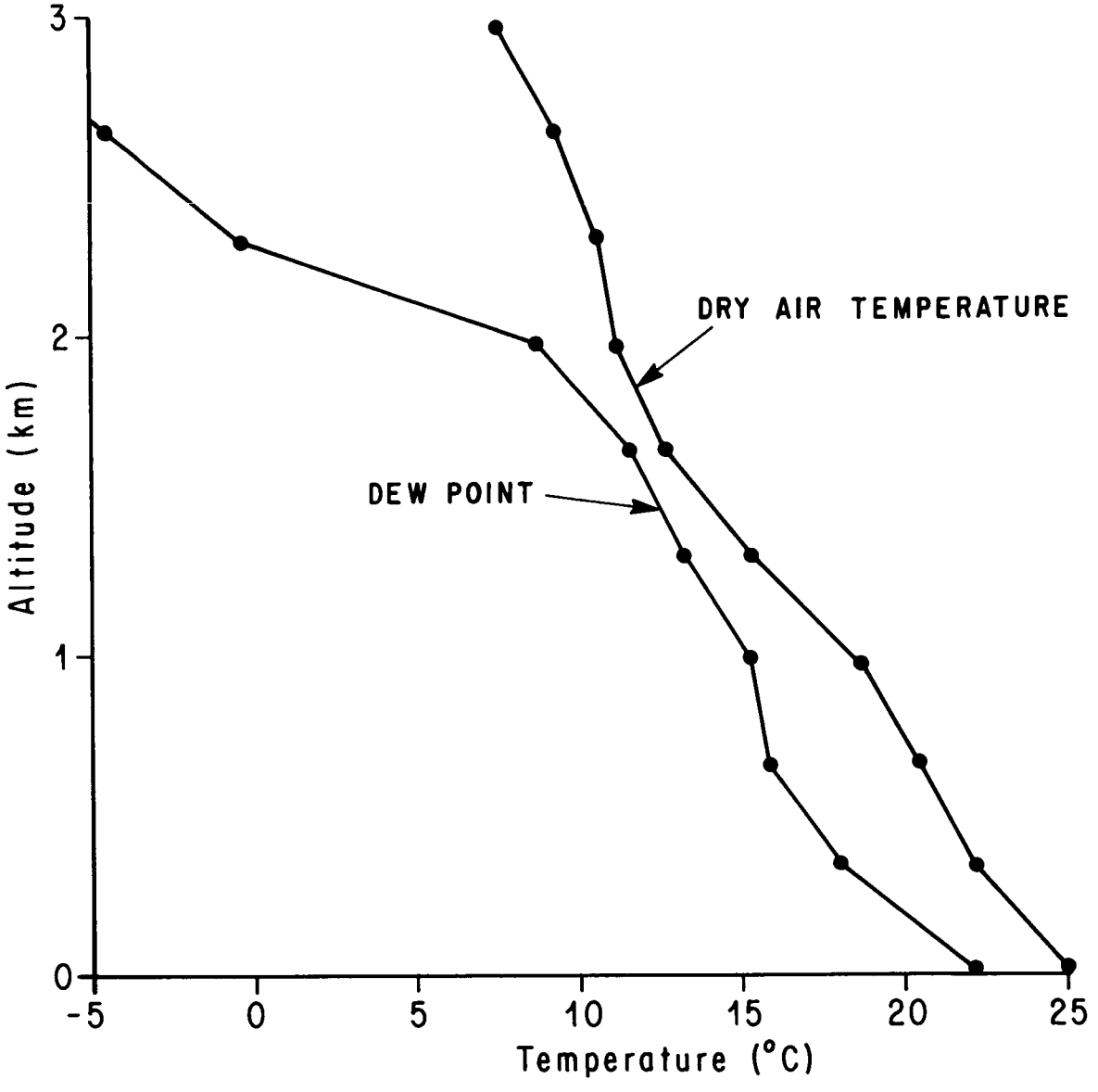

FIGURE 12. TEMPERATURE AND DEW-POINT PROFILES FROM THE 1430 UT RADIOSONDE SOUNDING ON AUGUST 13, 1972, WALLOPS ISLAND STATION, VIRGINIA

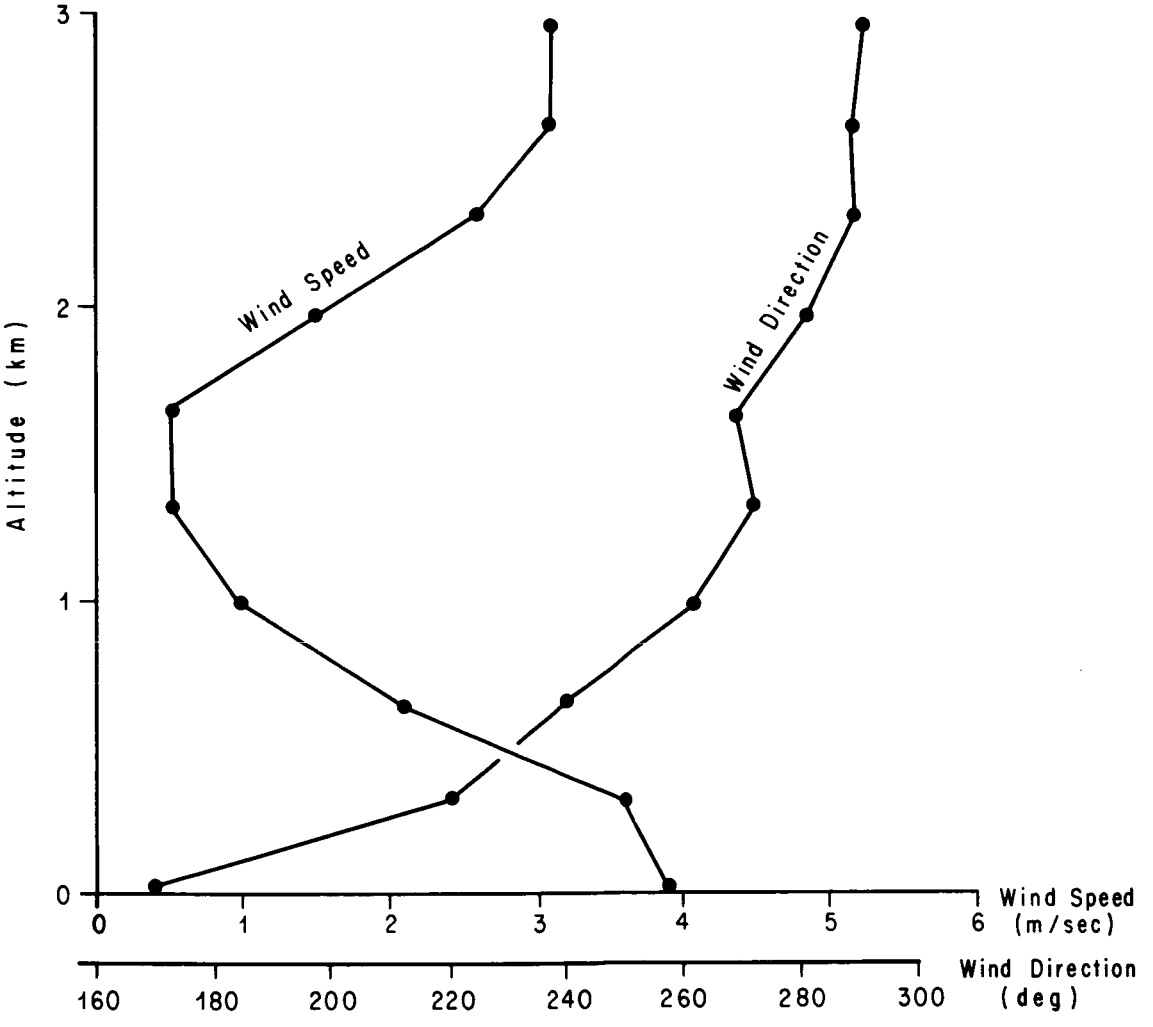

FIGURE 13. WIND SPEED AND DIRECTION PROFILES FROM THE 1430 UT RADIOSONDE SOUNDING ON AUGUST 13, 1972, WALLOPS ISLAND STATION, VIRGINIA

TABLE IX.

THE SCOUT-ALGOL III INPUT PARAMETERS TO PLUME RISE FORMULAS

A. General		
1. Initial cloud radius at the surface	r_R	0
2. Air density	ρ	167 g/m
3. Entrainment constant	γ_I	0.64
4. Specific heat of air at constant pressure	c_p	0.24 cal/g^{o}K
B. Meteorological Regime (1430UT, August 13, 1972)		
1. Ambient air temperature	T	298.16^{o}K
2. Vertical potential temperature gradient	$\frac{\partial\theta}{\partial z}$	0.005^{o}K/m

where g is the gravitational acceleration, T is the ambient temperature, and $\partial\theta/\partial z$ is the potential temperature gradient. The time required for the ground cloud to reach stabilization height was calculated to be 482 seconds for the parameters given in Table IX. The maximum height of cloud rise (Equation A-2) based on the 1430 UT sounding is 417 meters. This analytical prediction of the height compares well with the observed cloud rise heights (Figure 14) obtained using time-lapse photographs [5]. (While only a single analytically predicted cloud rise height has been determined, a predicted cloud rise curve can be analytically generated with Equation A-2.)

The height of cloud stabilization is then employed in the empirical prediction of the cloud diameter based on the MSFC library of cloud growth observations. The expression for the dimensions of the stabilized ground cloud is calculated as the standard deviation of the relative Lagrangian distance between two particles and is given by

$$\sigma_{zo} = \sigma_{yo} = \sigma_{xo} = \frac{\gamma_I \dot{z}_{mI}}{2.15} \qquad (6)$$

where σ_{zo}, σ_{yo}, and σ_{xo} are the vertical, crosswind and alongwind standard deviations for the dimensions. For the Scout-Algol III launch, the spherical entrainment leads directly to the above assumption of a symmetric stabilized ground cloud. The standard deviation for the predicted dimensions is 124 meters. For comparison of the predicted with observed cloud diameter, the photographically observed cloud growth as a function of time was made (Figure 15). The empirical cloud diameter, then, was determined to be 400 meters at an altitude of 417 meters (Figure 16). In the model for the source, the standard deviation for the source dimensions -- utilizing a Gaussian distribution -- implies that 95% of the material in the ground cloud was photographically visible compared to an expected 98%; that is, a 3% difference exists between the empirical results and the analytical results.

The ground cloud became stable with the ambient air 482 seconds after launch and had a maximum height of about 400 meters. At this time, the cloud contained 1592 kilograms of the rocket engine effluents from approximately the first 8 seconds of engine operation. It will be noted that the cloud stabilization time implied by the photographic analysis (Figures 14 and 15) is about 2 minutes; whereas, the analytic results obtained using Equation 5 is about 8 minutes. The differences between the empirical and analytical values obtained for the stabilization time and dimension are explainable using the following argument. The rate of change in the ground clouds growth and altitude follows an exponential decay as the point of stabilization is approached. The empirical values obtained through photographic analysis are limited in accuracy; therefore, empricial values obtained in this manner afford only about 80% of the

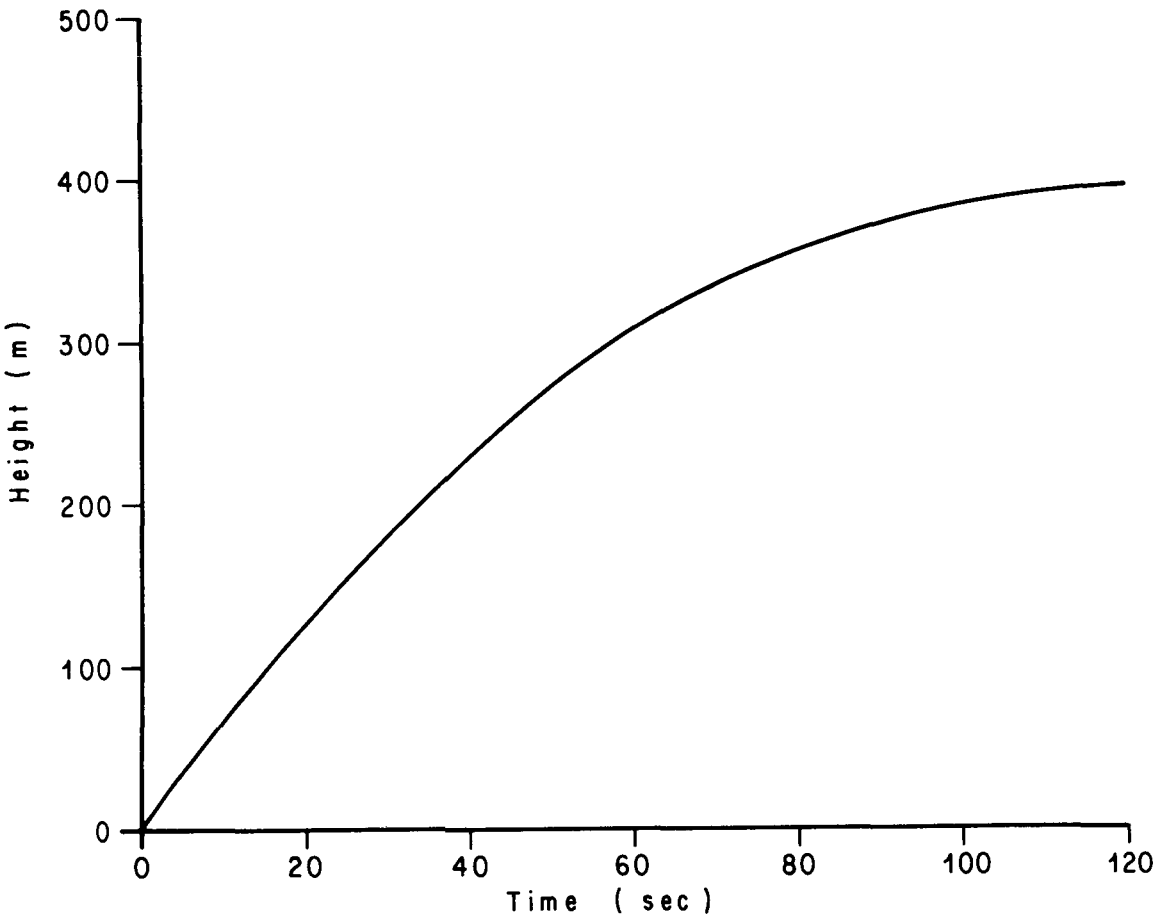

FIGURE 14. RISE RATE OF GROUND CLOUD FOR SCOUT VEHICLE LAUNCH AUGUST 13, 1972 (1510 UT) AT WALLOPS ISLAND, VIRGINIA OBTAINED FROM TIME LAPSE PHOTOGRAPHY

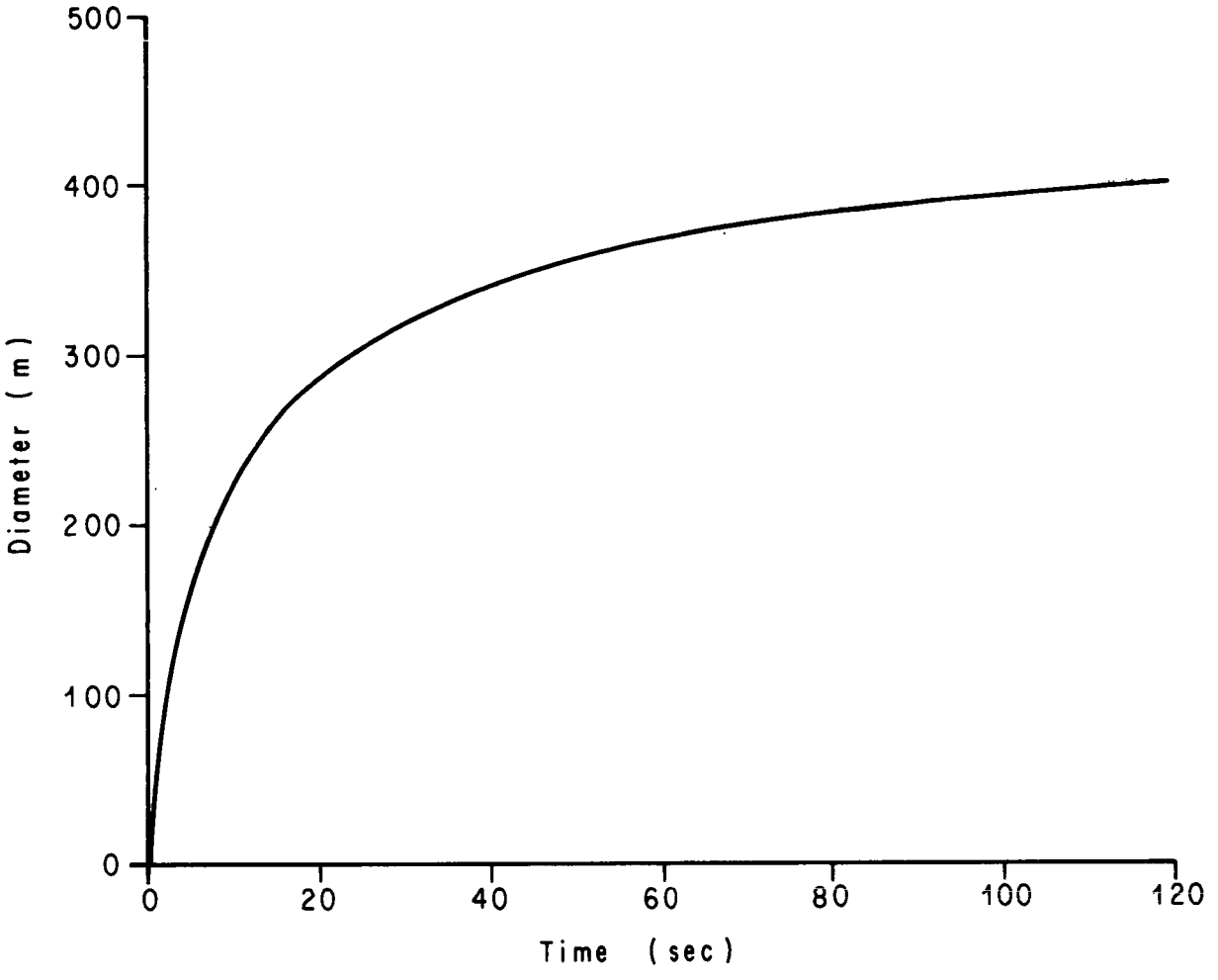

FIGURE 15. HORIZONTAL GROWTH OF GROUND CLOUD FOR SCOUT VEHICLE LAUNCHED ON AUGUST 13, 1972 (1510 UT) AT WALLOPS ISLAND, VIRGINIA OBTAINED FROM TIME LAPSE PHOTOGRAPHY

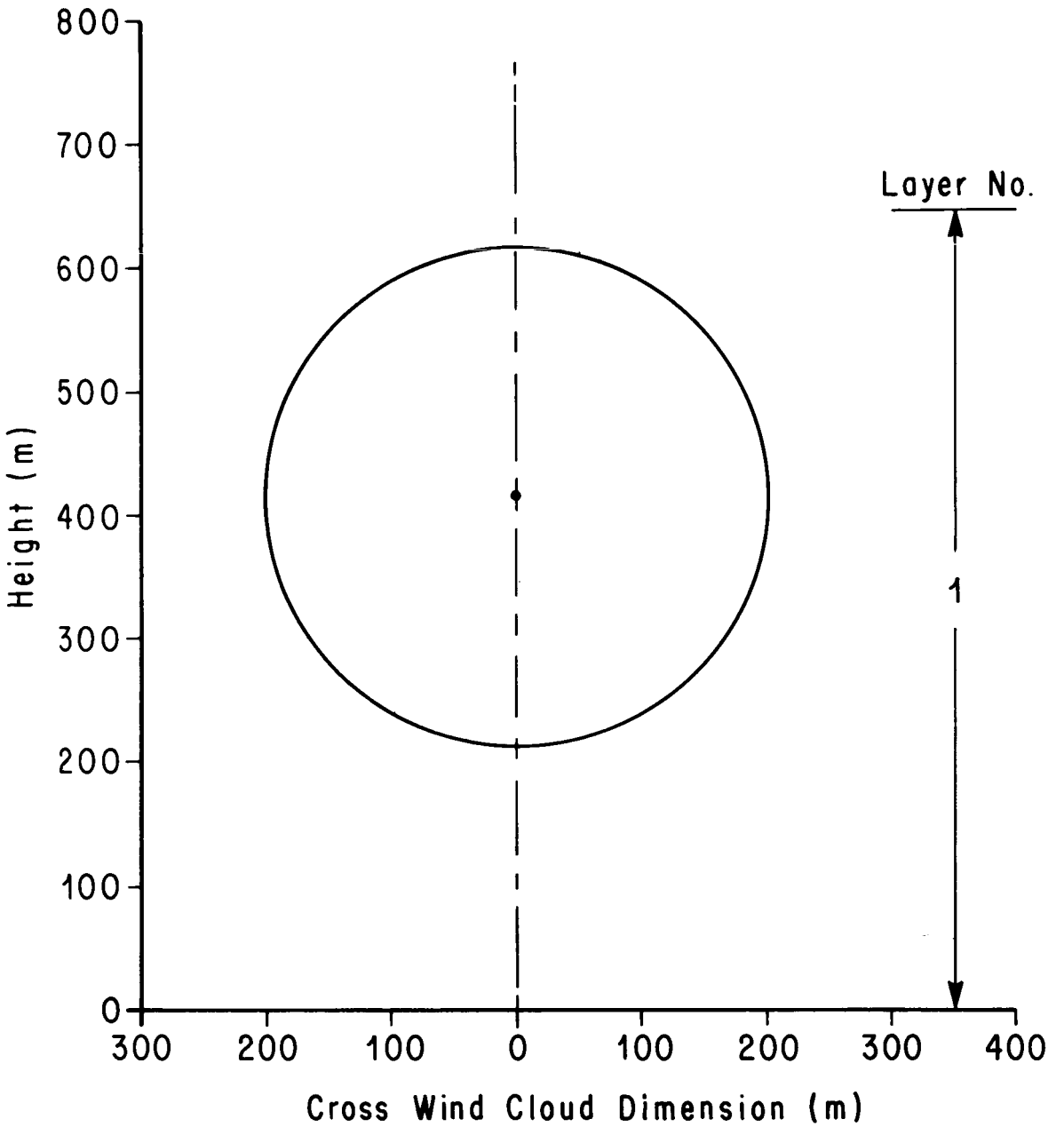

FIGURE 16. CROSS WIND AND VERTICAL DIMENSIONS ASSIGNED ANALYTICALLY TO THE GROUND CLOUD FORMED FROM SCOUT LAUNCH AT 1430 UT, AUGUST 13, 1972, AT WALLOPS ISLAND, VIRGINIA

total ground cloud development. This exponential decay of the growth is illustrated in the curve (Figure 17) of the rate's for the cloud radius to cloud altitude (r/z) as a function of time after launch. This ratio (r/z) is equal to the instantaneous entrainment coefficient (γ). The entrainment coefficient required in the cloud rise calculations is the average entrainment from launch to cloud stabilization, which is the average value of the entrainment. The cloud stabilization can be defined as the time when the instantaneous entrainment coefficient approaches a constant limiting value.

A detailed examination of the appropriate air temperature and dew point (Figure 12), and wind speed and direction (Figure 13) at the time of the launch of Scout-Algol III, on August 13, 1972, indicated the atmosphere should be treated as a single layer with regard to the ground cloud, rather than the nine layer model that was employed with Apollo 16. The NASA/MSFC Multilayer Diffusion Model 3 (spherical source) was applied to analyze the dispersive transport of effluents from the launch of the Scout-Algol III launch. (This model is summarized in the Section II and details for it are given in Appendix II.)

Source and meteorological input parameters for the NASA/MSFC Multilayer Diffusion Model are defined in Appendix III (Tables A-I and A-III). The values of the meteorological inputs, the source dimensions, and the source strength in the layer were obtained relative to the stabilized ground cloud (Figure 16) utilizing the relations in Appendix III (Equation A-39, A-40, and A-41). These meteorological and source input parameters (Table X) are the basis of the effluent dispersion results for the launch of the Scout-Algol III vehicle on August 13, 1972 that were obtained with the NASA/MSFC Multilayer Diffusion Model.

d. Predictions of the Centerline Concentration of Exhaust Effluents from the Launch of the Scout-Algol III, August 13, 1973, by use of the NASA/MSFC Multilayer Diffusion Model

The following predictions for the dispersion of the Algol III exhaust effluents from the Scout launch will focus on the dispersion of hydrogen chloride (HCl), carbon monoxide (CO) and alumina (Al_2O_3) because these are the only three constituents produced in significant amounts that are potentially toxic and have a potential impact on the environmental air quality in the troposphere. While carbon dioxide is produced and is potentially toxic, the amount is so small that it can be omitted from these discussions.

The results of the model calculations using Model 3 of the NASA/MSFC Multilayer Diffusion Model Program and the meteorological and source inputs in Table X are shown in Figures 18 through 20.

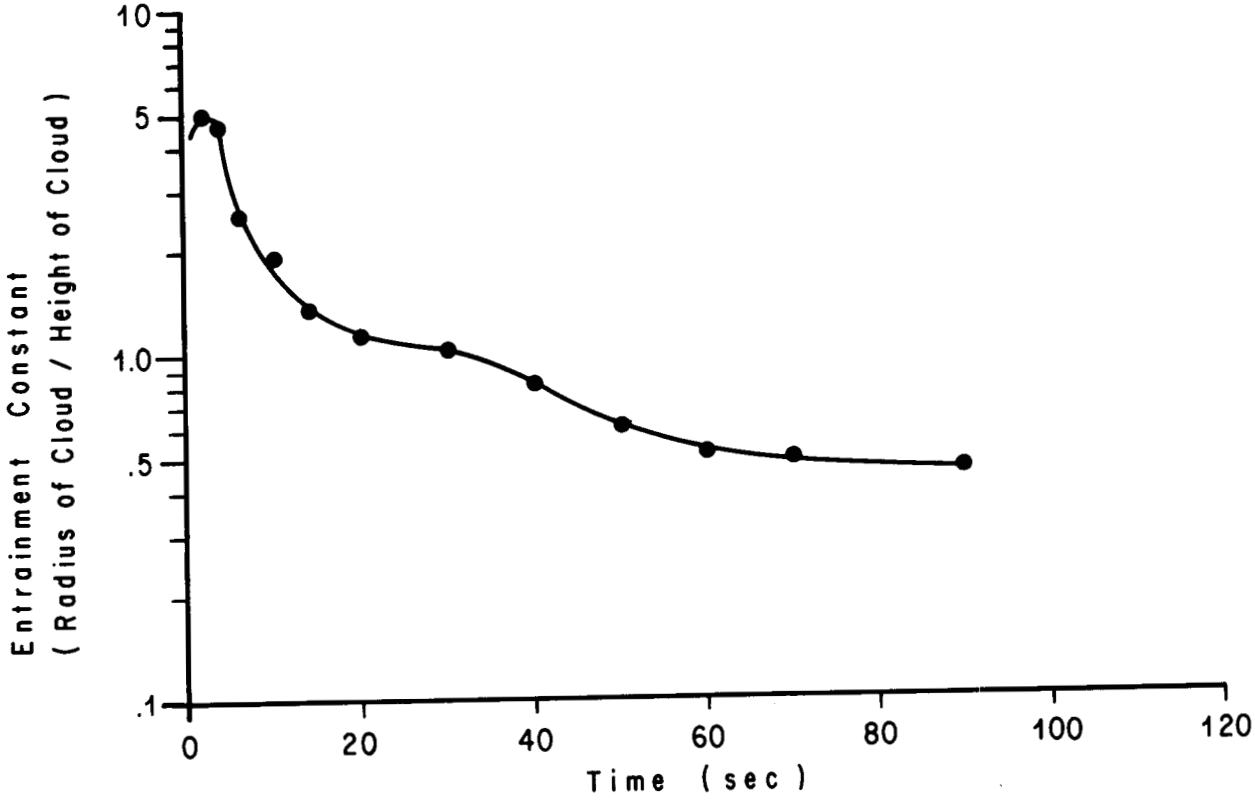

FIGURE 17. TIME DEPENDENT ENTRAINMENT COEFFICIENT FOR THE SCOUT VEHICLE

TABLE X.

METEOROLOGICAL AND SOURCE INPUT PARAMETERS FOR THE SCOUT-ALGOL III LAUNCH OF AUGUST 13, 1972

Parameter	Units	Model Input
Q_K - HCl	ppm m^3	2.153×10^8
CO	ppm m^3	3.730×10^8
Al_2O_3	mg	5.033×10^8
$\bar{u}_R$	m sec^{-1}	3.9
$\bar{u}_{TK}$	m sec^{-1}	1.43
z_{RK}	meters	2
$\sigma_{AR}\{\tau_{oK}\}$	degrees	5
$\sigma_{ATK}\{\tau_{oK}\}$	degrees	5
σ_{ER}	degrees	4.8
σ_{ETK}	degrees	4.8
τ_K	seconds	482
τ_{oK}	seconds	600
$\sigma_{xo} = \sigma_{yo} = \sigma_{zo}$	meters	124.13
α_K	dimensionless	1
β_K	dimensionless	1
z_{BK}	meters	0
z_{TK}	meters	1770
θ_{BK}	degrees	165
θ_{TK}	degrees	280
H_K	meters	417
x_{rz}	meters	100
x_{ry}	meters	100
x_{Rz}	meters	0
x_{Ry}	meters	0
z_K	meters	2; 417

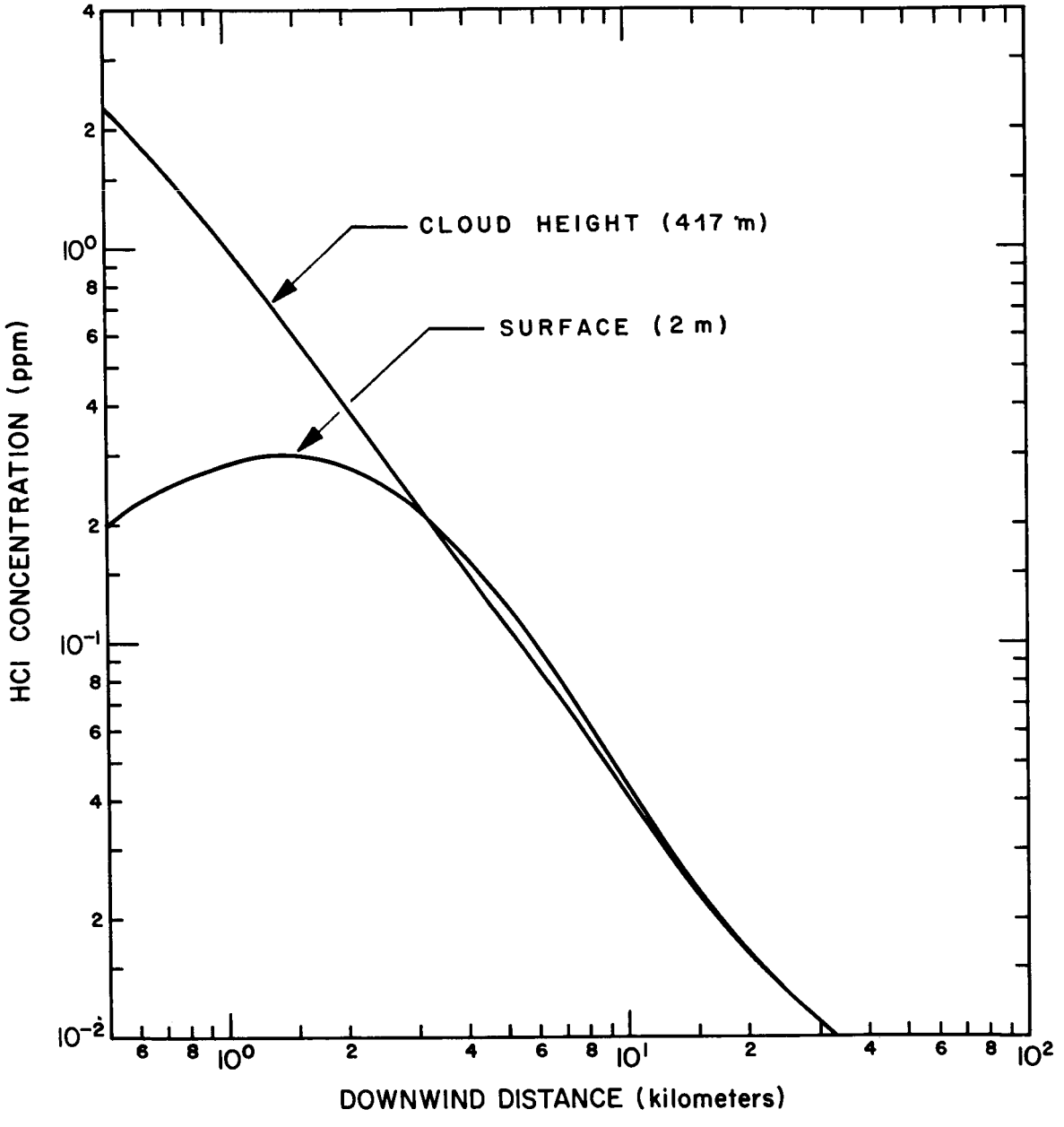

FIGURE 18. MAXIMUM CENTERLINE HCl CONCENTRATIONS NEAR THE SURFACE AND AT CLOUD STABILIZATION HEIGHT FOR THE SCOUT-ALGOL III LAUNCH OF AUGUST 13, 1972 AT WALLOPS ISLAND, VIRGINIA

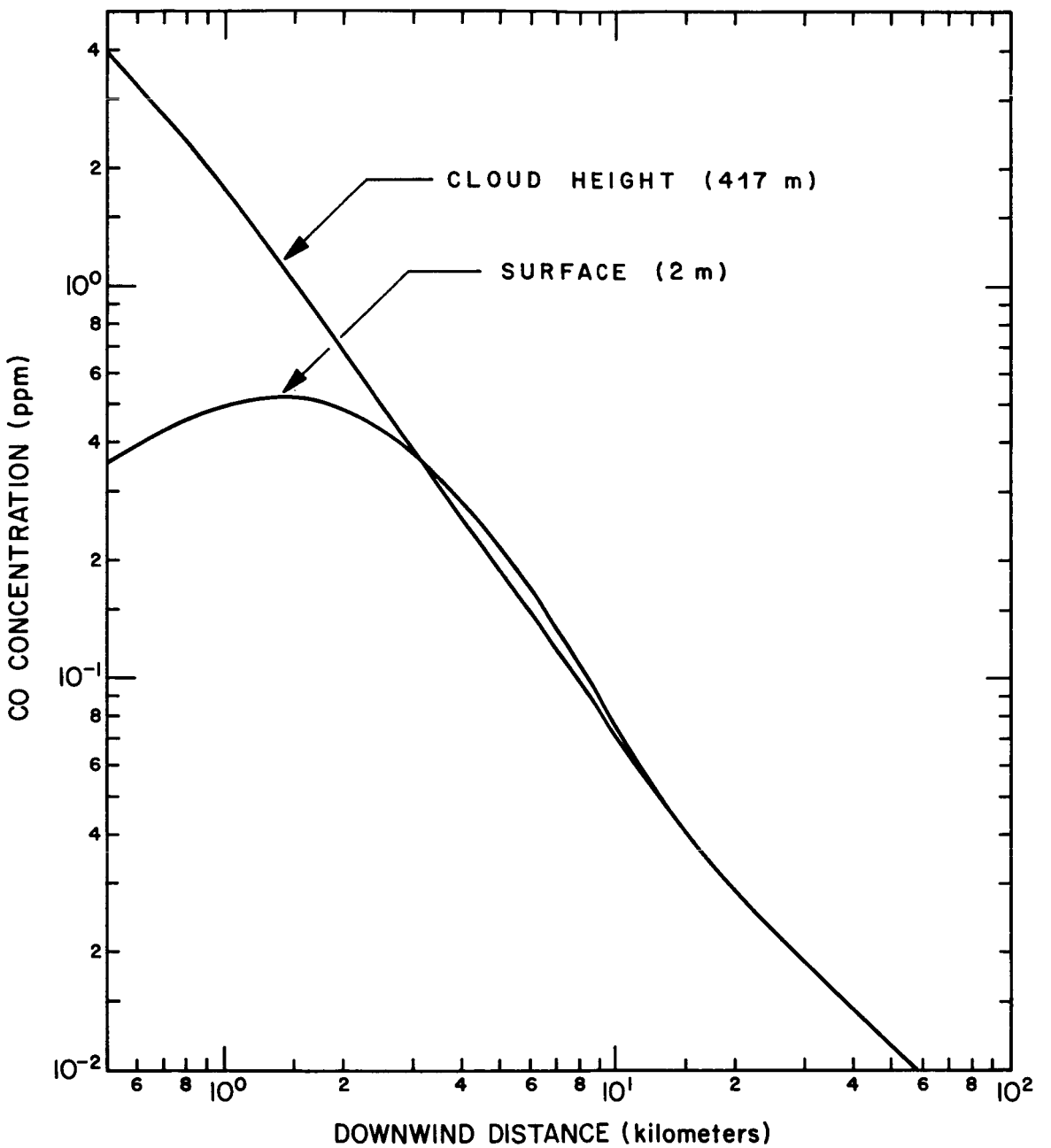

FIGURE 19. MAXIMUM CENTERLINE CO CONCENTRATIONS AT THE SURFACE AND AT CLOUD STABILIZATION HEIGHT FOR THE SCOUT-ALGOL III LAUNCH OF AUGUST 13, 1972 AT WALLOPS ISLAND, VIRGINIA

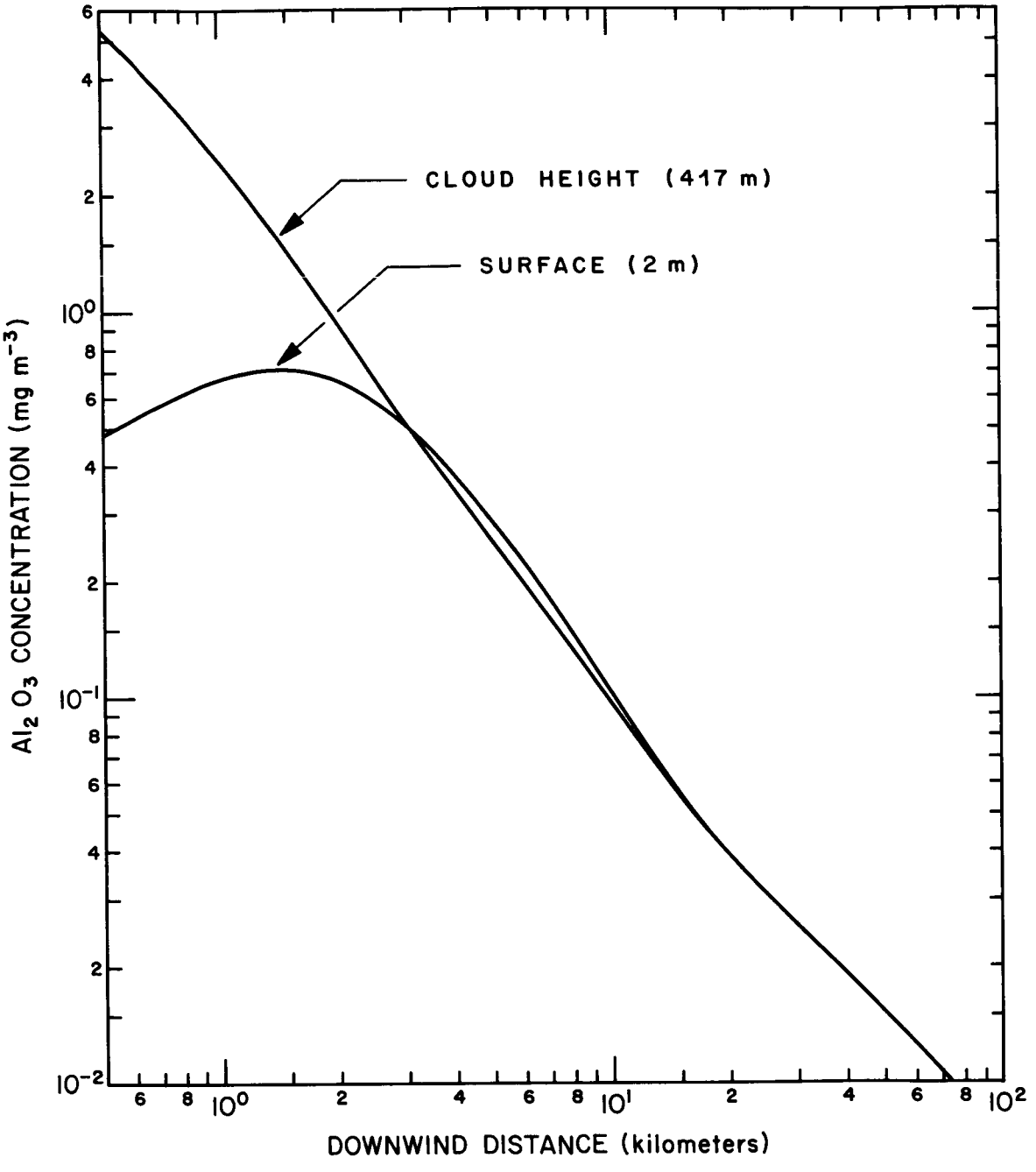

FIGURE 20. MAXIMUM CENTERLINE Al_2O_3 CONCENTRATIONS AT THE SURFACE AND AT CLOUD STABILIZATION HEIGHT FOR THE SCOUT-ALGOL III LAUNCH OF AUGUST 13, 1972 AT WALLOPS ISLAND, VIRGINIA

The maximum hydrogen chloride concentrations downwind from the Scout-Algol III launch of August 13, 1972 at a height of 2 meters above the surface and at the cloud stabilization height of 417 meters are given in Figure 18. Inspection of this figure shows that hydrogen chloride concentrations at 417 meters altitude decrease from about 2.3 parts per million near the source to less than 0.1 parts per million at a distance of 6 kilometers downwind from the source. Ground-level hydrogen chloride concentrations reach a maximum of about 0.3 parts per million about 1.5 kilometers downwind from the source. At distances beyond 3 kilometers from the source, the hydrogen chloride concentrations at the cloud stabilization height and the surface are nearly equal.

The concentrations of carbon monoxide and alumina were determined at the surface and at a height of 417 meters above the surface. Maximum concentrations of carbon monoxide at the ground surface do not exceed 0.52 parts per million (Figure 19) and for alumina do not exceed 0.7 milligrams per cubic meter (Figure 20). It should be noted that the calculation of alumina concentrations was made under the assumption that the alumina emitted by the Scout-Algol III vehicle consisted of finely divided particulates with no appreciable settling velocities.

The centerline concentrations at the surface and at the cloud stabilization altitude become approximately equal 3 kilometers downstream. This implies that the vertical distribution of effluents becomes uniform at this point and the dispersion of effluents is really being conducted as a Model 1 dispersion beyond this point in spite of the fact that Model 3 is being utilized.

The concentration levels for this Scout launch were at least a factor of approximately 10 less than the public exposure limits (Appendix IV). Due to the small amount of effluents from the Scout, the isopleths of the concentrations become meaningless; therefore, they have not been included.

APPENDIX I. CLOUD RISE FORMULA [1]

In order to determine whether an adiabatic or stable cloud rise relation should be utilized, it is necessary to determine the vertical potential temperature gradient $\left(\frac{\partial\theta}{\partial z}\right)$ which is described by

$$\frac{\partial\theta}{\partial z} = \frac{\theta}{T}\frac{\partial T}{\partial z} + \frac{g}{c_p} = \frac{\partial T}{\partial z} + \frac{g}{c_p} \tag{A-1}$$

where θ and T are the potential and ambient temperature, g is the gravitational acceleration, and c_p is the specific heat of air. If

$$\frac{\partial\theta}{\partial z} \leq 0 \tag{A-2}$$

the adiabatic cloud rise relation is used.

The maximum cloud rise z_{mI} downwind from an instantaneous source in an adiabatic atmosphere is given by

$$z_{mI} = \left[\frac{2 F_I t_{sI}^2}{\gamma_I^3 \bar{u}^2} + \left(\frac{r_R}{\gamma_I}\right)^4\right]^{1/4} - \frac{r_R}{\gamma_I} \tag{A-3}$$

whereas, the maximum cloud rise z_{mI} downwind from an instantaneous source in a stable atmosphere is given by

$$z_{mI} = \left[\frac{8F_I}{\gamma_I^3 s} + \left(\frac{r_R}{\gamma_I}\right)^4\right]^{1/4} - \frac{r_R}{\gamma_I} \tag{A-4}$$

where F_I is the instantaneous buoyancy parameter $\left(\frac{3gQ_I}{4\pi\rho c_p T}\right)$, Q_I is the effective heat released, ρ is the density of ambient air, γ_I is the entrainment coefficient, r_R is the initial cloud radius at the surface, s accounts for the vertical gradient of the potential temperature, and x_{sI} is the distance to reach stabilization. The subscript I means instantaneous and is used to flag a difference in the cloud rise models. The buoyancy terms, which is a function of the heat released and the type of entrainment, spherical and cylindrical, reflect the major difference in the two sources.

Equations (A-3) and (A-4) assume that the initial upward momentum imparted to the exhaust gases by reflection from the ground surface and launch pad hardware is insignificant in comparison with the thermal buoyancy flux. These relations are normally used with solid rocket motors.

The following formulas for the maximum buoyant rise of clouds from continuous sources are also based on procedures similar to those given by Briggs (1970). The maximum cloud rise z_{mc} downwind from a continuous source in an adiabatic atmosphere is given by

$$z_{mc} = \left[\frac{3 F_c x_{sc}^2}{2 \gamma_c^2 \bar{u}^3} + \left(\frac{r_R}{\gamma_c} \right)^3 \right]^{1/3} - \frac{r_R}{\gamma_c} \qquad \text{(A-5)}$$

The maximum cloud rise z_{mc} downwind from a continuous source in a stable atmosphere is given by

$$z_{mc} = \left[\frac{6 F_c}{\bar{u} \gamma_c^2 s} + \left(\frac{r_R}{\gamma_c} \right)^3 \right]^{1/3} - \frac{r_R}{\gamma_c} \qquad \text{(A-6)}$$

where F_c is the continuous buoyancy flux parameter and is equal to $\frac{gQ_c}{\pi \rho c_p T}$. The subscript c implies that the associated parameter is unique to the continuous source. The primary difference in these continuous source relations is that the temperature constraint in the stable atmosphere results in a buoyancy damping.

Equations (A-5) and (A-6) assume that the initial momentum flux imparted to the cloud by dynamic forces is negligible in comparison buoyancy flux. Again, experience in calculating cloud rise for normal launches of large liquid fueled rockets and for static firings has shown that this assumption is reasonable [6-10].

APPENDIX II. CONCENTRATION-DOSAGE FORMULATION FOR NASA/ MSFC MULTILAYER DIFFUSION MODEL

The fundamental relation for the concentration-dosage calculation will be presented for the ellipsoidal source used in Model 3. These relations are appropriate to the elliptic-cylindrical distribution of Model 1 if the vertical dispersive interaction is neglected. This part of the Appendix is complex; therefore, only recommended when a detailed scientific knowledge is required.

The dosage equation for Model 3 in the K-th layer is given by the expression

$$D_K\{x_K, y_K, z_{BK} < z_K < z_{TK}\} = \frac{Q_K}{2\pi\,\sigma_{yK}\,\sigma_{zK}\,\bar{u}_K} \left\{ \exp\left[\frac{-y_K^2}{2\sigma_{yK}^2}\right] \right\}$$

$$\left\{ \exp\left[\frac{-(H_K - z_K)^2}{2\sigma_{zK}^2}\right] + \exp\left[\frac{-(H_K - 2z_{BK} + z_K)^2}{2\sigma_{zK}^2}\right] \right.$$

$$+ \sum_{i=1}^{\infty} \left\{ \exp\left[\frac{-\left(2i\,(z_{TK} - z_{BK}) - (H_K - 2z_{BK} + z_K)\right)^2}{2\sigma_{zK}^2}\right] \right. \qquad \text{(A-7)}$$

$$\exp\left[\frac{-\left(2i\,(z_{TK} - z_{BK}) + (H_K - z_K)\right)^2}{2\sigma_{zK}^2}\right] + \exp\left[\frac{-\left(2i\,(z_{TK} - z_{BK}) - (H_K - z_K)\right)^2}{2\sigma_{zK}^2}\right]$$

$$\left. \left. + \exp\left[\frac{-\left(2i\,(z_{TK} - z_{BK}) + (H_K - 2z_{BK} + z_K)\right)^2}{2\sigma_{zK}^2}\right] \right\} \right\}$$

where Q_K corresponds to the source strength or total mass of material in the layer and H_K is the height of the centroid of the stabilized cloud.

The standard deviation of the vertical dosage distribution (σ_{zK}) is defined by the expression

$$\sigma_{zK} = \sigma'_{EK}\, x_{rzK} \left(\frac{x_K + x_{zK} - x_{rzK}(1-\beta_K)}{\beta_K\, x_{rzK}} \right)^{\beta_K} \qquad \text{(A-8)}$$

where σ'_{EK} describes the mean standard deviation of the wind elevation angle, x_{zK} gives the vertical virtual distance, β_K accounts for vertical diffusion, and x_{rzK} is the distance over which rectilinear vertical expansion occurs downwind from an ideal point source in the K-th layer.

In the surface layer (K = 1), the standard deviation of the wind elevation angle (σ_{ER}) at the height z_R is described by

$$\sigma_{EK}\{K=1\} = \frac{\sigma_{ER}\left[\left(z_{TK}\{K=1\}\right)^{q+1} - \left(z_R\right)^{q+1}\right]}{\left(q+1\right)\left(z_{TK}\{K=1\} - z_R\right)\left(z_R\right)^{q}} \left(\frac{\pi}{180}\right) \quad \text{(A-9)}$$

where the power-law exponent (q) for the vertical profile of the standard deviation of the wind elevation angle in the surface layer is

$$q = \log\left(\frac{\sigma_{ETK}\{K=1\}}{\sigma_{ER}}\right) \Big/ \log\left(\frac{z_{TK}\{K=1\}}{z_R}\right) \quad \text{(A-10)}$$

here $\sigma_{ETK}\{K=1\}$ is the standard deviation of the wind elevation angle at the top of the surface layer. Above the surface layer (K>1), the standard deviation of the wind elevation angle is

$$\sigma'_{EK}\{K>1\} = \left(\sigma_{ETK} + \sigma_{EBK}\right)\left(\frac{\pi}{360}\right) \quad \text{(A-11)}$$

where σ_{ETK} and σ_{EBK} are the standard deviations of the wind elevation angle at the top and the base of the layer.

The vertical virtual distance x_{zK} is given by the expression

$$\begin{cases} \dfrac{\sigma_{zo}\{K\}}{\sigma'_{EK}} - x_{RzK} & ; \ \sigma_{zp}\{K\} \le \sigma'_{EK}\, x_{rzK} \\ \beta_K\, x_{rzK}\left(\dfrac{\sigma_{zo}\{K\}}{\sigma'_{EK}\, x_{rzK}}\right)^{1/\beta_K} - x_{RzK} + x_{rzK}(1-\beta_K) & ; \ \sigma_{zo}\{K\} \ge \sigma'_{EK}\, x_{rzK} \end{cases} \quad \text{(A-12)}$$

where $\sigma_{zo}\{K\}$ is the standard deviation of the vertical dosage distribution at x_{RzK}, the distance from the source where the measurement is made in the K-th layer.

The remaining terms are common also to Model 1; that is, what has just been discussed is to account for the vertical expansion of the source cloud.

The quantity $\bar{u}_K$ in Equation (A-7) is the mean cloud transport speed in the K-th layer. In the surface layer (K=1), the wind speed-height profile is defined according to the power-law expression

$$\bar{u}\left\{z_K,\ K=1\right\} = \bar{u}_R\left(\frac{z_K\{K=1\}}{z_R}\right)^p \qquad \text{(A-13)}$$

where $\bar{u}_R$ is the mean wind speed measured at the reference height z_R and the power-law exponent (p) for the wind speed profile in the surface layer is described by

$$p = \log\left(\frac{\bar{u}_{TK}\{K=1\}}{\bar{u}_R}\right)\Bigg/\log\left(\frac{z_{TK}\{K=1\}}{z_R}\right) \qquad \text{(A-14)}$$

here $\bar{u}_{TK}\{K=1\}$ corresponds to the mean wind speed at the top of the surface layer $\left(z_{TK}\{K=1\}\right)$. Thus, in the surface layer, the mean cloud transport speed ($u\{K=1\}$) is

$$\bar{u}_K\{K=1\} = \frac{\bar{u}_R}{\left(z_{TK}\{K=1\} - z_R\right) z_R{}^p}\int_{z_R}^{z_{TK}}\left(z_K\{K=1\}\right)^p\,dz \qquad \text{(A-15)}$$

which reduces to

$$\bar{u}_K\{K=1\} = \frac{\bar{u}_R\left[\left(z_{TK}\{K=1\}\right)^{1+p} - \left(z_R\right)^{1+p}\right]}{\left(z_{TK}\{K=1\} - z_R\right)\left(z_R\right)^p\left(1+p\right)} \quad . \qquad \text{(A-16)}$$

In layers above the surface layer (K>1), the wind speed-height profile $\left(\bar{u}\{z_K, K>1\}\right)$ is assumed linear and defined as

$$\bar{u}\left\{z_K, K>1\right\} = \bar{u}_{BK} + \left(\frac{\bar{u}_{TK} - \bar{u}_{BK}}{z_{TK} - z_{BK}}\right)\left(z_K - z_{BK}\right) \qquad \text{(A-17)}$$

where $\bar{u}_{TK}$ and $\bar{u}_{BK}$ describe the mean wind speed at the top of the layer and at the base of the layer, respectively. In the K-th layer (K>1), the mean cloud transport speed $\left(\bar{u}_K\{K>1\}\right)$ is

$$\bar{u}_K\{K>1\} = \left(\bar{u}_{TK} + \bar{u}_{BK}\right)/2 \qquad \text{(A-18)}$$

The standard deviation of the crosswind dosage distribution $\left(\sigma_{yK}\right)$ is defined by

$$\sigma_{yK} = \left\{ \left[\sigma'_{AK}\{\tau_K\}\, x_{ryK} \left(\frac{x_K + x_{yK} - x_{ryK}\left(1-\alpha_K\right)}{\alpha_K\, x_{ryK}} \right)^{\alpha_K} \right]^2 + \left[\frac{\Delta\theta'_K\, x_K}{4.3} \right]^2 \right\}^{1/2} \qquad \text{(A-19)}$$

where $\sigma'_{AK}\{\tau_K\}$ corresponds to the mean layer standard deviation of the wind azimuth for the cloud stabilization time $\left(\tau_K\right)$. In the surface layer (K=1),

$$\sigma'_{AK}\{\tau_K, K=1\} = \frac{\sigma'_{AR}\{\tau_K\}\left[\left(z_{TK}\{K=1\}\right)^{m+1} - \left(z_R\right)^{m+1}\right]}{\left(m+1\right)\left(z_{TK}\{K=1\} - z_R\right)\left(z_R\right)^m} \qquad \text{(A-20)}$$

where the standard deviation of the wind azimuth angle $\left(\sigma'_{AR}\{\tau_K\}\right)$ at height z_R and for the cloud stabilization time τ_K is

$$\sigma'_{AR}\{\tau_K\} = \sigma_{AR}\{\tau_{oK}\}\left(\frac{\tau_K}{\tau_{oK}}\right)^{1/5}\left(\frac{\pi}{180}\right) \qquad \text{(A-21)}$$

here $\sigma_{AR}\{\tau_{oK}\}$ is the standard deviation of the wind azimuth angle at height z_R and for the reference time period $\left(\tau_{oK}\right)$, and the power-law exponent (m) for the vertical profile of the standard deviation of the wind azimuth angle in the surface layer is

$$m = \log\left(\frac{\sigma'_{ATK}\{\tau_K, K=1\}}{\sigma'_{AR}\{\tau_K\}}\right) \Big/ \log\left(\frac{z_{TK}\{K=1\}}{z_R}\right) . \qquad \text{(A-22)}$$

Then

$$\sigma'_{ATK}\{\tau_K, K=1\} = \sigma_{ATK}\{\tau_{oK}, K=1\} \left(\frac{\tau_K}{\tau_{oK}}\right)^{1/5} \left(\frac{\pi}{180}\right) \qquad \text{(A-23)}$$

where $\sigma_{ATK}\{\tau_{oK}, K=1\}$ is the standard deviation of the wind azimuth angle at the top of the surface layer for the reference time period. For layers above the surface (K>1),

$$\sigma'_{ATK}\{\tau_K, K>1\} = \left(\sigma'_{ATK}\{\tau_K\} + \sigma'_{ABK}\{\tau_K\}\right) \Big/ 2 \qquad \text{(A-24)}$$

where

$$\sigma'_{ATK}\{\tau_K\} = \sigma_{ATK}\{\tau_{oK}\} \left(\frac{\tau_K}{\tau_{oK}}\right)^{1/5} \left(\frac{\pi}{180}\right) \qquad \text{(A-25)}$$

here $\sigma_{ATK}\{\tau_{oK}\}$ is the standard deviation of the wind azimuth angle at the top of the layer.

$$\sigma'_{ABK}\{\tau_K\} = \sigma_{ABK}\{\tau_{oK}\} \left(\frac{\tau_K}{\tau_{oK}}\right)^{1/5} \left(\frac{\pi}{180}\right) \qquad \text{(A-26)}$$

here $\sigma_{ABK}\{\tau_{oK}\}$ is the standard deviation of the wind azimuth angle in degrees at the base of the layer for the reference time period $\left(\tau_{oK}\right)$.

The crosswind virtual distance is

$$x_{yK} = \frac{\sigma_{yo}\{K\}}{\sigma'_{AK}\{\tau_K\}} - x_{RyK} \qquad \text{(A-27)}$$

$$\text{when } \sigma_{yo}\{K\} \leq \sigma'_{AK}\{\tau_K\}\, x_{ryK}$$

or

$$x_{yK} = \alpha_K\, x_{ryK} \left(\frac{\sigma_{yo}\{K\}}{\sigma'_{AK}\{\tau_K\}\, x_{ryK}} \right)^{1/\alpha_K} - x_{RyK} + x_{ryK}(1-\alpha_K) \qquad \text{(A-28)}$$

$$\text{when } \sigma_{yo}\{K\} \geq \sigma'_{AK}\{\tau_K\}\, x_{ryK}$$

here $\sigma_{yo}\{K\}$ is the standard deviation of the lateral source dimension in the layer at downwind distance x_{RyK}, x_{ryK} is the distance over which rectilinear crosswind expansion occurs downwind from an ideal point source, and α_K describes the lateral diffusion in the layer. The vertical wind direction shear $\left(\Delta\theta'_K\right)$ in the layer is

$$\Delta\theta'_K = \left(\theta_{TK} - \theta_{BK}\right)\left(\frac{\pi}{180}\right) \qquad \text{(A-29)}$$

where θ_{TK} and θ_{BK} are the mean wind direction at the top, and at the base of the layer, respectively.

The concentration algorithm is of the same form for the first three models; however, the dosage term $\left(D_K\right)$ does depend on which model has been utilized, and thus adjusts the concentration description to the specific model of interest.

The maximum concentration for the first three models in the K-th layer is given by the expression

$$\chi_K\{x_K, y_K, z_K\} = \frac{D_K\, \bar{u}_K}{\sqrt{2\pi}\, \sigma_{xK}} \qquad \text{(A-30)}$$

where the standard deviation of the alongwind concentration distribution $\left(\sigma_{xK}\right)$ in the layer is

$$\sigma_{xK} = \left[\left(\frac{L\{x_K\}}{4.3}\right)^2 + \sigma_{xo}^2\{K\}\right]^{1/2} \qquad \text{(A-31)}$$

and the alongwind cloud length $\left(L\{x_K\}\right)$ for a point source in the layer at the distance x_K from the source is

$$L\{x_K\} = \left\{ \begin{array}{ll} \dfrac{0.28\left(\Delta\bar{u}_K\right)\left(x_K\right)}{\bar{u}_K} & ; \quad \Delta\bar{u}_K \geq 0 \\ 0 & ; \quad \Delta\bar{u}_K \leq 0 \end{array} \right\} \qquad \text{(A-32)}$$

where $\Delta\bar{u}_K$ is the vertical wind speed shear in the layer and is defined as

$$\Delta\bar{u}_K\{K=1\} = \bar{u}_{TK}\{K=1\} - \bar{u}_R \qquad \text{(A-33)}$$

or

$$\Delta\bar{u}_K\{K>1\} = \bar{u}_{TK} - \bar{u}_{BK} \qquad \text{(A-34)}$$

and $\sigma_{xo}\{K\}$ is the standard deviation of the alongwind source dimension in the layer at the point of cloud stabilization. The above equation for $L\{x_K\}$ is based on the theoretical and empirical results reported by Tyldesley and Wallington (1967) [11] who analyzed ground-level concentration measurements made at distances of 5 to 120 kilometers downwind from instantaneous line-source releases.

The maximum centerline concentration for the model in the K-th layer is given by the expression

$$\chi_{CK}\{x_K, y_K=0, z_K\} = \chi_K / \{\text{LATERAL TERM}\} \qquad \text{(A-35)}$$

The average alongwind concentration is defined as

$$\bar{\chi}_K = D_K / t_{pK} \qquad \text{(A-36)}$$

where the ground cloud passage time in seconds is

$$t_{pK} \cong 4.3\ \sigma_{xK} / \bar{u}_K \qquad \text{A-37)}$$

The time mean alongwind concentration in the K-th layer is defined by the expression

$$\chi_K\{x_K, y_K, z_K; T_A\} = \frac{D_K}{T_A} \left\{ \operatorname{erf}\left(\frac{\bar{u}_K\ T_A}{2\sqrt{2}\ \sigma_{xK}} \right) \right\} \qquad \text{(A-38)}$$

where T_A is the time in seconds over which concentration is to be averaged. The time mean alongwind concentration is equivalent to the average alongwind concentration when t_{pK} equals T_A. This complex set of relations, then, are the computations performed in Model 3 to obtain the concentration-dosage mappings.

APPENDIX III. INPUT PARAMETERS FOR THE NASA/MSFC MULTILAYER DIFFUSION MODEL

There are to groups of input parameters for the model. The source input parameters which are vehicle and meteorologically dependent (Table A-I) and the meteorological input parameters which are strictly dependent on meteorological conditions at launch time (Table A-II). These parameters include the special set employed in the layer breakdown model -- Model 4.

The source relationships given in Table A-I are determined in reference to the stabilized ground cloud. The standard deviation of the crosswind source is

$$\sigma_{yo}\{K\} = \frac{Y\{K\}}{4.3} \tag{A-39}$$

and the standard deviation of the alongwind source is

$$\sigma_{xo}\{K\} = \frac{X\{K\}}{4.3} \tag{A-40}$$

The source strength in the K-th layer is

$$Q_K = \left(\frac{Y\{K\}\ X\{K\}}{\Sigma Y\{K\}\ X\{K\}}\right) \quad \frac{Q_T}{z_{TK} - z_{BK}} \tag{A-41}$$

where $Y\{K\}$ and $X\{K\}$ describe the crosswind and alongwind dimensions of the cloud in the K-th layer, and Q_T is the total source strength in the ground cloud in units of mass.

Equations (A-39) and (A-40) are based on the assumption that the alongwind and crosswind distribution of material in each layer is Gaussian and that the visible edge of the cloud represents the point at which the concentration is one-tenth the concentration at the cloud center in the K-th layer. Equation (A-41) assumes that the cloud is spheroidal in the plane of the horizon and that the total source strength in the K-th layer is given by the relative cloud volume in the K-th layer. Because the models require the source strength per unit height, the total source strength in the K-th layer must be divided by the depth of the layer.

The first nine meteorological parameters follow directly from the thermodynamic and kinematic profiles of the atmosphere. The remaining two parameters (layer model) are empirical atmospheric constants.

TABLE A-I

SOURCE INPUTS FOR THE MULTILAYER MODEL CALCULATIONS

PARAMETER		DEFINITION
Layer Model 1, 2, 3	Layer Breakdown Model: 4	
z_R	z_R	Reference height in the surface layer
z_{BK}	z_{BL}	Height of the layer base
z_{TK}		Height of the layer top
τ_K	τ_L	Source (cloud) stabilization time
x_{ryK}	x_{ryL}	Distance over which rectilinear lateral expansion occurs downwind from an ideal point source
$\sigma_{yo}\{K\}$		Standard deviation of the crosswind source dimension in the K-th layer
$\sigma_{xo}\{K\}$		Standard deviation of the alongwind source dimension in the K-th layer
	t^*	Time of layer breakdown
Q_K		Source strength in the layer
J		Scaling coefficient

TABLE A-II

LIST OF METEOROLOGICAL MODEL INPUTS

PARAMETER		DEFINITION
Layer Model: 1, 2, 3	Layer Breakdown Model: 4	
$\bar{u}_R$	$\bar{u}_{RL}$	Mean wind speed at reference height z_R
$\bar{u}_{BK}$	$\bar{u}_{BL}$	Mean wind speed at the base of the layer
$\bar{u}_{TK}$	$\bar{u}_{TL}$	Mean wind speed at the top of the layer
θ_{BK}	θ_{BL}	Mean wind direction at the base of the layer
θ_{TK}	θ_{TL}	Mean wind direction at the top of the layer
$\sigma_{AR}\{\tau_{oK}\}$	$\sigma_{ARL}\{\tau_{oL}\}$	Standard deviation of the wind azimuth angle at height z_R
$\sigma_{ABK}\{\tau_{oK}\}$	$\sigma_{ABL}\{\tau_{oL}\}$	Standard deviation of the wind azimuth angle at the base of the layer
$\sigma_{ATK}\{\tau_{oK}\}$	$\sigma_{ATL}\{\tau_{oL}\}$	Standard deviation of the wind azimuth angle at the top of the layer
τ_{oK}	τ_{oL}	Reference time period
α_K	α_L	Lateral diffusion coefficient
$p\{K=1\}$	$p\{L=1\}$	Power-law exponent of the wind speed profile in the surface layer
	σ_{ERL}	Standard deviation of the wind elevation angle at height z_R
	σ_{EBL}	Standard deviation of the wind elevation angle at the base of the L-th layer
	σ_{ETL}	Standard deviation of the wind elevation angle at the top of the L-th layer
	β_L	Vertical diffusion coefficient

APPENDIX IV. TOXICITY CRITERIA

Realistic evaluation of the potential hazard arising from high near-field concentrations of toxic effluents from solid rocket exhaust requires both a knowledge of the surface deposition of these effluents -- which can be obtained with the MSFC/NASA Multilayer Diffusion Model (Appendix II), and a toxicity criteria to evaluate the hazard from this surface deposition of effluent -- which is the incumbency for this discussion. The Federal Air Quality Criteria does not presently include any of the liquid or solid rocket exhaust effluents; however, the National Academy of Sciences does afford definite guidelines for the exposure to the toxic effluents associated with these exhausts. These guidelines are ecologically sound, based on the current limited knowledge of the effects of these effluents, and are the basis of the toxicity criteria that will be given [12, 13].

The primary effluents from any solid rocket exhaust are: aluminum oxide, (Al_2O_3), hydrogen chloride (HCl), carbon monoxide (CO), carbon dioxide (CO_2), hydrogen (H_2), nitrogen (N_2) and water vapor (H_2O). While only the first four compounds are toxic in significant concentrations, there is always a potential hazard of suffocation from any gas which results in the reduction of the partial pressure of oxygen to a level below 135 mm Hg (18% by volume at STP). Oxygen level reduction does not appear to be a hazard from rocket exhaust due to the large volume of air which is entrained into these exhaust clouds; therefore, this potential hazard can be neglected in this discussion and the attention directed to only the initial four toxic compounds. (A liquid rocket motor has only one toxic effluent -- carbon monoxide.)

The exposure level for toxic effluents are divided into three categories: public exposure level, emergency public exposure level, and occupational exposure level. The public exposure levels are designed to prevent any detrimental health effects both to all classes of human beings (children, men, women, the elderly, those of poor healt, etc.) and to all forms of biological life. The emergency level is designed as a limit in which some detrimental effects may occur, especially, to biological life. The occupational level gives the maximum allowable concentration which a man in good health can tolerate -- this level could be hazardous to various forms of biological life.

The toxicity criteria for the toxic effluents in solid rocket exhausts are given in Table A-III. Public health levels for aluminum oxide are not given because the experience with these particulate is so limited that, at best, the industrial limits are just good estimates.

TABLE A-III. AIR QUALITY TOXICITY STANDARDS**

TOXIC SOLID ROCKET EXHAUST PRODUCT	TIME INTERVAL (MINUTES)	CONCENTRATION		
		PUBLIC	EMERGENCY	OCCUPATIONAL
		***		
Alumina (Al_2O_3)	10	5.0 mg/m^3	x	50 mg/m^3
	30	2.5 mg/m^3	x	25 mg/m^3
	60	1.5 mg/m^3	x	15 mg/m^3
	480	1.0 mg/m^3	x	10 mg/m^3
Hydrogen Chloride (HCl)	10	4 ppm	7 ppm	30 ppm
	30	2 ppm	3 ppm	20 ppm
	60	2 ppm	3 ppm	10 ppm
Carbon Monoxide (CO)	10	90 ppm	275 ppm	1000 (1500*) ppm
	30	35 ppm	100 ppm	500 (800*) ppm
	60	25 ppm	66 ppm	200 (400*) ppm
DOSAGE:		200 ppm/ time interval		
Carbon Dioxide (CO_2)	480	x	x	Average - 5000 ppm
		x	x	Peak - 6250 ppm

Parts of vapor or gas per million parts of contaminated air by volume at 25°C and 760 mm Hg.

**These values were reviewed on the phone by Ralph C. Wands, Director Advisory Center on Toxicology, National Academy of Sciences, 2101 Constitution Avenue, Washington, D. C. 20418, April 1973.

*At these concentrations, headaches will occur along with a loss in work efficiency.

***EPA suggests a safety factor of ten (10) to be applied to occupational exposure limits [

Hydrogen chloride is an irritant; therefore, the concentration criterion for an interval should not be exceeded [13]. Since hydrogen chloride is detrimental to biological life, and in view of the fact that most launch sites are encompassed by wild life refuges, the emergency and industrial criteria for hydrogen chloride are not appropriate to the ecological constraints. Because of the large volume of air entrained in the exhaust cloud, the potential hazard from carbon monoxide and carbon dioxide can be, in general, neglected.

Any detrimental health effects due to combined toxicological action of these ingredients has been omitted because of a lack of knowledge in this area. However, investigations are currently underway to study this problem and to learn more about the biological effects of hydrogen chloride.

REFERENCES

1. Dumbauld, R. K., J. R. Bjorklund, and J. F. Bowers: NASA/MSFC Multilayer Diffusion Models and Computer Program for Operational Prediction of Toxic Fuel Hazards. Report under Contract No. NAS8-29033. TR-73-201-02, March 1973.

2. Laudau, L. D. and E. M. Lifshitz: Fluid Mechanics, Volume 6 of Course of Theoretical Physics, Pergamon Press, 1959.

3. Susko, Michael, John W. Kaufman, and Kelly Hill: Rise Rate and Growth of Static Test Vehicle Engine Exhaust Clouds, NASA TM X-53782, pp 146-166, October 15, 1968.

4. Thayer, Scott D., Martin W. Chandler, and Roland T. Chu: Rise and Growth of Space Vehicle Engine Exhaust and Associated Diffusion Models. NASA CR-61331, July 1970.

5. Susko, Michael and J. W. Kaufman, "Exhaust Cloud Rise and Growth for Apollo Saturn Engines, Journal of Spacecraft and Rockets, May 1973.

6. Briggs, G. A., "Some Recent Analyses of Plume Rise Observations," Paper presented at the 1970 International Union of Air Pollution Prevention Associations, Atmospheric Turbulence and Diffusion Laboratory, National Oceanic and Atmospheric Administration, Oak Ridge, Tennessee, USA, ATDL, No. 38, 1970.

7. Hanna, Steven R., "Cooling Tower Plume Rise and Condensation" Paper presented at Air Pollution Turbulence and Diffusion Symposium, Las Cruces, New Mexico, December 7-10, 1971.

8. Smith, Michael R. and Richard E. Forbes, "Mass-Energy Balance for an S-IC Rocket Exhaust Cloud During Static Firing," NASA CR-61357, August 4, 1971.

9. Church, H. W., "Cloud Rise from High-Explosives Detonations," TID-45000 (53rd Ed) UC-41, Health & Safety, SC-RR-68-903, Sandia Laboratories, Albuquerque, June 1969.

10. Tucker, G. L. Maj., H. E. Malone, and Capt. R. W. Smith, "Atmospheric Diffusion of Beryllium - Project Adobe" Report No. AFRPL-TR-70-65, Three Volumes, Director of Laboratories, Air Force System Command, July 1971.

11. Tyldesley, J. B. and C. E. Wallington, The Effect of Wind Shear and Vertical Diffusion on Horizontal Dispersion. Quart. J. Roy. Met. Soc., 91, 1967, 158-174.

REFERENCES (Continued)

12. National Primary and Secondary Ambient Air Quality Standards, Environmental Protection Agency, Part II of Federal Register, Vol. 36, No. 84, April 1971 (Updated Nov. 1971).

13. "Guides for Short-Term Exposures of the Public to Air Pollutants, Vol. II. Guide for Hydrogen Chloride, "Committee on Toxicology of the National Academy of Sciences - National Research Council, Washington, D. C., August 1971

NASA-Langley, 1973 —— 13